

Chloride Regulation: A Dynamic Equilibrium Crucial for Synaptic Inhibition

Nicolas Doyon,^{1,2} Laurent Vinay,³ Steven A. Prescott,^{4,5} and Yves De Koninck^{1,6,*}

¹Institut Universitaire en Santé Mentale de Québec, Québec, QC G1J 2G3, Canada

²Department of Mathematics and Statistics, Université Laval, Québec, QC G1V 0A6, Canada

³Team P3M, Institut de Neurosciences de la Timone, UMR 7289, CNRS and Aix Marseille Université, F-13385 Marseille, France

⁴Program in Neurosciences and Mental Health, Hospital for Sick Children, Toronto, ON M5G 1X8, Canada

⁵Department of Physiology, University of Toronto, Toronto, ON M5S 1A8, Canada

⁶Department of Psychiatry and Neuroscience, Université Laval, Québec, QC, G1V 0A6, Canada

*Correspondence: yves.dekoninck@neuro.ulaval.ca
<http://dx.doi.org/10.1016/j.neuron.2016.02.030>

Fast synaptic inhibition relies on tight regulation of intracellular Cl^- . Chloride dysregulation is implicated in several neurological and psychiatric disorders. Beyond mere disinhibition, the consequences of Cl^- dysregulation are multifaceted and best understood in terms of a dynamical system involving complex interactions between multiple processes operating on many spatiotemporal scales. This dynamical perspective helps explain many unintuitive manifestations of Cl^- dysregulation. Here we discuss how taking into account dynamical regulation of intracellular Cl^- is important for understanding how synaptic inhibition fails, how to best detect that failure, why Cl^- regulation is energetically so expensive, and the overall consequences for therapeutics.

Effective synaptic inhibition is crucial for proper neural coding. Beyond preventing runaway excitation within recurrently connected networks like cortex, inhibition enables efficient and effective coding by producing oscillations in neural activity, restricting receptive field size, sharpening tuning, and regulating dynamic range through gain modulation (Chance et al., 2002; Green and Swets, 1988; Isaacson and Scanziani, 2011; Marr, 1982; Prescott and De Koninck, 2003; Seriès et al., 2003; Soto-Treviño et al., 2001; Viemari et al., 2011). Consistent with the diverse and important roles played by inhibition, neural coding is degraded when and if synaptic inhibition is disrupted in any way. The list of neurological disorders in which disruption of synaptic inhibition is implicated is long and continually growing (Boulenguez et al., 2011; Coull et al., 2003; Ferrini et al., 2013; Hewitt et al., 2009; Huberfeld et al., 2007; Hyde et al., 2011; Khubieh et al., 2015; Price et al., 2005).

Fast inhibition in the central nervous system is mediated primarily by Cl^- currents through GABA_A and glycine-gated receptors/channels. The strength and polarity of those Cl^- currents depend not only on the activation of ligand-gated channels, they also depend on the electrochemical gradient that drives Cl^- through the channels when they open (Ben-Ari et al., 2012; Buzsáki et al., 2007; De Koninck, 2007). To be precise, synaptic inhibition relies on Cl^- flowing down its gradient and into the cell, even in the case of shunting inhibition (see “The Ebb and Flow of Chloride,” below). This influx of Cl^- would necessarily deplete the electrochemical Cl^- gradient were the gradient not constantly replenished by other mechanisms. Loss of inhibitory efficacy can result from reduced activation of GABA_A/glycine receptors and/or depletion of the Cl^- gradient, but the result is not exactly the same in each case. Those differences can provide valuable insights into the root cause of the disinhibition; conversely, identifying the mechanisms underlying disinhibition can help predict precisely how (e.g., under what circumstances)

inhibition will fail, how best to detect such failure, and how to prevent or reverse such failures when they occur.

In this Review, we will discuss the link between Cl^- dysregulation and the diminished capacity of inhibitory synaptic input to reduce neuronal spiking. The decrease in inhibitory function is often referred to as *disinhibition*; notably, the same term is also used to describe active inhibition of inhibitory neurons such that downstream neurons are released from inhibition. We will use the term exclusively in the former context. We will place special emphasis on the importance of treating Cl^- regulation as a dynamical system comprising multiple interacting processes. Indeed, Cl^- driving force is typically assumed to remain constant on the short timescale of other physiological processes but, under pathological conditions, $[\text{Cl}^-]$ can change quite rapidly, slower than a single synaptic event but fast enough to change during a barrage of synaptic inputs or during sustained GABA_A or glycine receptor activation; under such conditions, Cl^- driving force cannot be legitimately treated as constant and must, rather, be treated as a dynamic variable.

After introducing the fundamental processes that contribute to setting intracellular Cl^- levels, we will address why the interaction between those processes is so important. For instance, we will explain why the same change in Cl^- extrusion capacity can cause a small or large change in the GABA/glycine reversal potential (E_{anion}) depending on Cl^- load. This is important for understanding under what conditions synaptic inhibition will fail when compromised by Cl^- dysregulation, and specifically that increased inhibitory synaptic transmission tends to exacerbate disinhibition rather than temper it. The same issues are important for designing experiments that are maximally sensitive to small reductions in Cl^- extrusion capacity, and for reappraising past experiments which were insensitive to such changes. We will also discuss the impact of Cl^- regulation on energy consumption, showing that modes of Cl^- regulation which maintain low

$[Cl^-]_i$, such as high levels of KCC2 activity, lead to significantly more energy consumption than modes of Cl^- regulation related to higher levels of $[Cl^-]$. We discuss how this greater energy consumption is associated with improved synaptic signaling and how synaptic signaling suffers when Cl^- extrusion is reduced. Lastly, we will discuss how the intricacies of Cl^- dynamics can determine the success or failure of therapeutic strategies. Specifically, emerging drugs targeting the activity of transporters offer promising alternatives to drugs targeting the conductance of inhibitory channels (Brumback and Staley, 2008; Ferrini et al., 2013; Gagnon et al., 2013; Kahle et al., 2014a).

The Ebb and Flow of Chloride

GABA_A and glycine receptor/channels are permeable to Cl^- and, to a lesser extent, bicarbonate (HCO_3^-) (Kaila, 1994; Staley and Proctor, 1999; Staley et al., 1995). The binding of ligands to the receptor opens a central pore, thus enabling anions to move through the channel. The direction of ion flux is dictated by the underlying electrochemical gradient for each ion. The electrochemical gradient constitutes the driving force, which corresponds to the difference between the membrane potential and the reversal potential for a given ion. The reversal potential in turn depends on the relative concentration of ions inside and outside the neuron, as described by the Nernst equation (E_{Cl} is in the -85 mV to -70 mV range in healthy adult neurons, while E_{HCO_3} is more depolarized, in the -40 mV to -20 mV range [Arosio et al., 2010; Kaila, 1994]). For most mature neurons in the CNS, intracellular Cl^- is maintained at a low concentration of around 5 mM , which is why Cl^- normally flows into the neuron (based on the driving force) when GABA_A or glycine receptors are activated. Bicarbonate ions flow in the opposite direction, offsetting some of the outward (i.e., hyperpolarizing) current produced by Cl^- influx. When relating current flow and ion flux, one should recall that the direction of current is defined by the movement of positive charge, which is why *influx* of chloride anions constitutes an *outward* current.

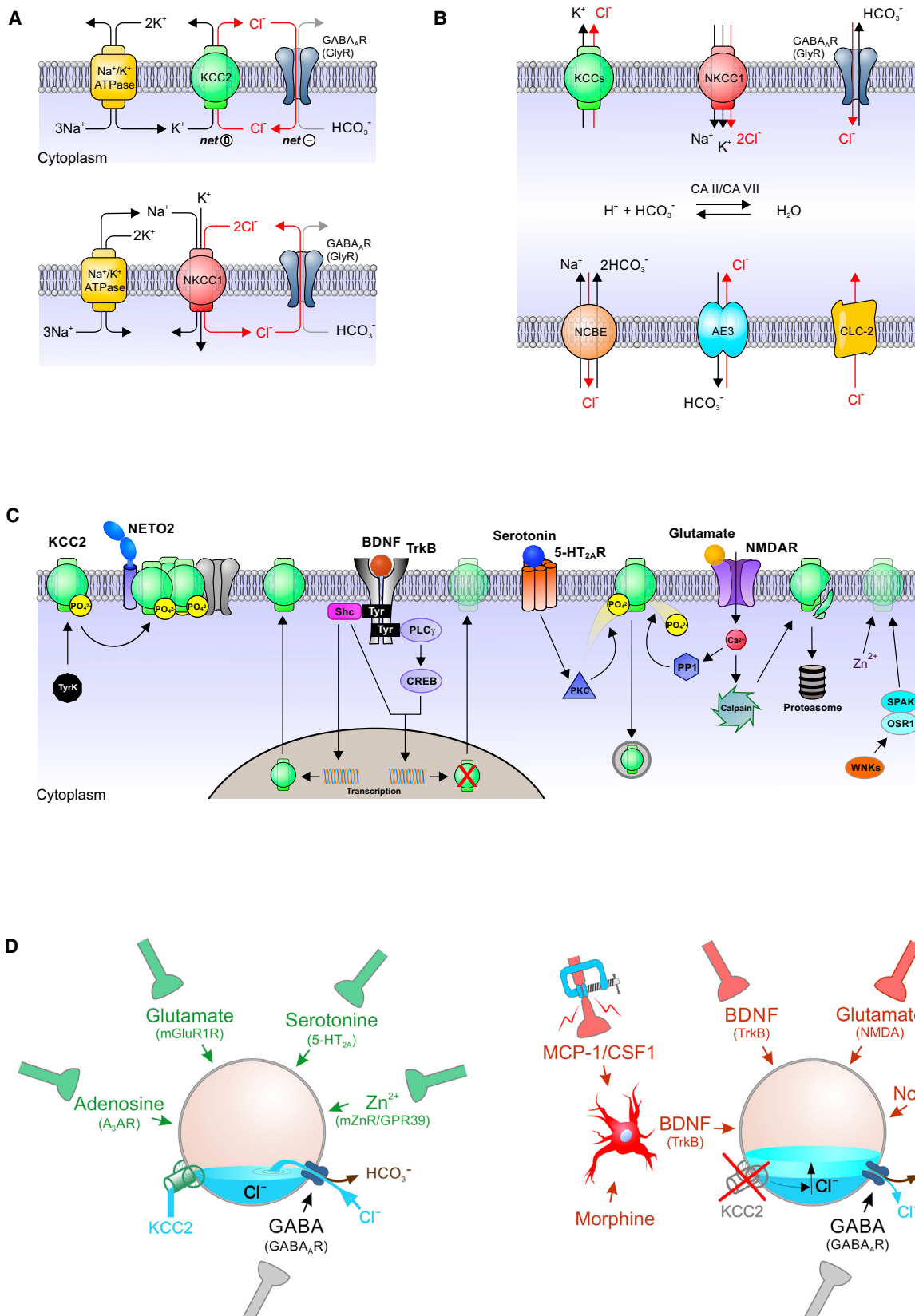
In mature neurons, Cl^- is maintained at a low intracellular level primarily through the actions of a K^+ - Cl^- cotransporter known as KCC2 (Figure 1A) (Ben-Ari et al., 2012; Kaila et al., 2014; Payne et al., 2003; Williams and Payne, 2004). KCC2 moves Cl^- against its gradient, extruding it from inside the cell by allowing Cl^- to piggyback K^+ as the latter moves down the K^+ electrochemical gradient. The overall process is electroneutral and does not directly involve energy consumption; instead, the cotransport process utilizes the electrochemical K^+ gradient whose maintenance involves the sodium-potassium ATPase, which is energy dependent (Figure 1A). KCC2 appears to be the main Cl^- extruder expressed by neurons and is solely expressed in the CNS (Payne et al., 2003; Williams et al., 1999). That said, other transport processes are involved in shuttling Cl^- across the membrane, most notably Na^+ - K^+ - Cl^- cotransporter NKCC1, which loads Cl^- into the cell. These cation-chloride cotransporters (CCCs) and other transporters such as NCC, NCBE, and Cl^-/HCO_3^- exchangers (Figure 1B) implicate a number of other ions whose regulation thus becomes inextricably tied up with Cl^- regulation. Regulation of pH, for example, impacts inhibition because of the involvement of bicarbonate in both processes and because of the Cl^- - HCO_3^- exchanger

(Doyon et al., 2011). Even membrane depolarization is important insofar as it affects driving force independent of any direct change in E_{anion} (Doyon et al., 2016). It should also be noted that Cl^- diffuses within the intracellular space, moving from areas of high concentration into areas of lower concentration, as well as away from fixed negative charges, which is important for redistributing Cl^- load on fast timescales (Brumback and Staley, 2008; Doyon et al., 2011; Kuner and Augustine, 2000; Raimondo et al., 2012).

$GABA_A$ and glycine receptors are often said to mediate shunting inhibition because the reversal potential (E_{anion}), which can be computed through the Goldman-Hodgkin-Katz equation and is in essence a weighted mean of E_{Cl} and E_{HCO_3} according to the respective ionic permeabilities, is close to the resting membrane potential. This terminology refers to the fact that activating $GABA_A$ or glycine receptors does not cause overt hyperpolarization in a cell at rest but, instead, mitigates (i.e., shunts) depolarization caused by concurrent excitatory input. This so-called shunting effect occurs because outward current flowing through $GABA_A$ /glycine receptors counteracts the inward current flowing through glutamate receptors. This in turn means that, contrary to what is often thought, inhibition in such a case does involve Cl^- influx and, therefore, imposes a Cl^- load on the inhibited neuron (Prescott, 2015). Stronger outward current confers stronger inhibition, but this comes at the cost of a stronger Cl^- load (see “Activity-Dependent Disinhibition” below).

This means that synaptic inhibition imposes a Cl^- load on the neuron, and that the efficacy of synaptic inhibition in turn relies on mechanisms to counteract that Cl^- load. $[Cl^-]_i$ is therefore in dynamic equilibrium. A static view of Cl^- regulation implies that parameters such as the strength of CCC activity and cation gradients determine a fixed value of $[Cl^-]_i$, which, in turn, defines the strength of inhibition. However, the dynamical equilibrium of Cl^- involves processes working on different timescales, which means that changes in $[Cl^-]_i$ are not simple (i.e., linear) and never occur in isolation; instead, the component processes interact nonlinearly to produce complex dynamics. These must be taken into account to properly predict the impact of manipulating inhibition (see “Pathological Implications and Lessons for Therapeutics” below).

Adding to this, there is mounting evidence that KCC2, which is primarily responsible for maintaining low $[Cl^-]_i$ in adult tissue and for restoring low $[Cl^-]_i$ following a Cl^- load, is itself modulated by an array of intracellular and intercellular signaling mechanisms. Intracellular regulatory mechanisms include transcriptional and posttranscriptional processes. The latter involve phosphorylation/dephosphorylation mechanisms, recycling, cleavage, interactions with molecular partners affecting membrane and intracellular trafficking, quaternary structure (oligomerization), and possibly distribution within membrane microdomains (lipid rafts) (Figure 1C; for recent reviews, see Kahle et al., 2013; Kahle and Delpey, 2015; Kaila et al., 2014; Medina et al., 2014; Watanabe and Fukuda, 2015; Wu et al., 2015). Intercellular signaling mechanisms regulating KCC2 expression/function include BDNF acting on TrkB receptors, 5HT acting on 5HT2A receptors, glutamate acting on NMDA receptors (and perhaps mGluRs), noradrenaline, Zn^{2+} acting on mZnR/GPR39 receptors, and perhaps even adenosine acting on A3AR receptors (Figure 1D; Bos et al., 2013; Coull



(legend on next page)

et al., 2003; Ferrini and De Koninck, 2013; Ferrini et al., 2013; Ford et al., 2015; Gilad et al., 2015; Hewitt et al., 2009; Lee et al., 2011).

These regulatory processes impact Cl^- homeostasis through a sort of *metahomeostasis*. The parameters of Cl^- homeostasis are found to change in different conditions, notably throughout development and in pathological conditions. Many variables are thus involved in shaping the complexity of inhibition and determining how it is controlled. With this in mind, the remainder of this paper focuses on practical insights gleaned by treating Cl^- regulation as a rich, nonlinear dynamical process.

Activity-Dependent Disinhibition

The amplitude of GABA_A receptor-mediated inhibitory postsynaptic current (IPSC) was long ago observed to decrease during high-frequency stimulation (Huguenard and Alger, 1986; Thompson and Gähwiler, 1989). This results from the Cl^- that enters the cell through synaptic channels accumulating intracellularly because its clearance by KCC2 is rate limited (orders of magnitude slower than flow through Cl^- channels) (Brumback and Staley, 2008; Doyon et al., 2011; Kaila, 1994). The relationship between Cl^- load, Cl^- extrusion, and Cl^- accumulation is schematically illustrated in Figure 2A. Cl^- accumulation is especially large and rapid in small compartments, like dendrites, where the surface area to volume ratio is large and diffusion is restricted by the small radius and large distance from the soma. When present at sufficient levels, KCC2 can deal with sizeable Cl^- loads (e.g., extrusion rate in dendrites have been reported on the order of 5 mM/s) (Staley and Proctor, 1999), but it can still be overwhelmed by atypically large floods of Cl^- , such as might occur pathologically or experimentally. While this has been shown in a variety of experimental contexts, we illustrate this principle using a simple computational model (e.g., a Morris-Lecar model extended to include $[\text{Cl}^-]$ dynamics) (Doyon et al., 2016) (Figures 2B and 2C). Importantly, if KCC2 function is tested under conditions in which the neuron experiences little or no Cl^- load, a large decrease in KCC2 function could go undetected (Figure 2B) (see also “The Mismeasure of Chloride Regulation” below). But that is not to say that only large reductions in KCC2 are functionally relevant; on the contrary, since neurons can experience sizeable Cl^- loads under normal conditions, even small reductions in KCC2 can be consequential. It is likely that subtle reductions

in KCC2 function have been overlooked in past studies because those studies did not test KCC2 function under in vivo-like Cl^- load conditions. As we will discuss below, subtle reductions in KCC2 can have significant consequences for neural coding.

The History Dependence of Failing Inhibition

Two important consequences of disinhibition resulting from reduced Cl^- extrusion capacity are (1) increased lability (i.e., larger fluctuations) in steady state $[\text{Cl}^-]$; and (2) slower convergence of $[\text{Cl}^-]$ to its steady state when Cl^- load fluctuates due to changes in GABA_A or glycine receptor activation (Figure 2C) (Doyon et al., 2016). These two factors play important roles in determining how a neuron responds to a barrage of inhibitory synaptic inputs. If a burst of synaptic inputs occurs in a dendrite, the small volume of the compartment and limited diffusion capacity cause rapid Cl^- accumulation ($[\text{Cl}^-]$ increases on the order of 20 mM can occur within hundreds of milliseconds), which decreases the strength of IPSCs (Figure 3A, right panels) (Brumback and Staley, 2008; Doyon et al., 2011; Kaila, 1994; Raimondo et al., 2012). In these small compartments, some Cl^- accumulation will transiently occur even with strong KCC2 expression. Strong Cl^- extrusion can nonetheless mitigate Cl^- accumulation and prevent the inversion of IPSCs into paradoxically depolarizing events. In contrast, at the level of the soma, because of the dramatically larger volume (the rate of Cl^- accumulation is given by $I_{\text{Cl}}/(F \cdot \text{Vol})$ where F is the Faraday constant and Vol is the effective volume of the neuronal compartment), KCC2 activity can prevent a collapse in IPSC strength (Figure 3A, left panels). In either case, Cl^- extrusion capacity impacts both the extent and the rate of change in IPSC strength. The fact that IPSC strength depends upon input history has been referred to as an ionic plasticity (Raimondo et al., 2012; Rivera et al., 2005). While in many sensory systems adaption diminishes the transmission of sustained or repeated stimuli, Cl^- ionic plasticity produces exactly the opposite by causing inhibition to progressively weaken. This activity-dependent disinhibition thus counteracts any weakening of the excitatory input. Ionic plasticity can also cause a dissociation between the amount of inhibitory synaptic transmission and the degree of functional inhibition; in other words, the same GABA or glycine release will induce postsynaptic currents whose amplitude varies on the basis of events occurring seconds earlier. Such activity-dependent

Figure 1. Cl^- Homeostasis and Metahomeostasis

(A) Schematic of Cl^- and HCO_3^- flow through GABA_A /glycine channels; shuttling of Na^+ , K^+ , and Cl^- through the cation-chloride cotransporters (CCCs) KCC2 and NKCC1; and the relationship to ATP consumption. The Cl^- to HCO_3^- permeability ratio for GABA_A /glycine channels is 4:1, such that in normal conditions the net result is a negative charge flowing in (i.e., a net outward current; expressed as the direction of positive charge flow). In contrast, ion transport through these CCCs is electroneutral (no net charge or current).

(B) Summary of the major sources of Cl^- influx and efflux in neurons. The direction of Cl^- flow through CIC-2 channels has been debated because of the channel's rectification properties, but since Cl^- flux is dictated by the electrochemical Cl^- gradient, CIC-2 channels let Cl^- leak into the neuron, not out (Ratté and Prescott, 2011). Only in conditions where the electrochemical gradient for Cl^- is reversed does CIC-2 serve to extrude Cl^- (Staley, 1994).

(C) Schematic diagram illustrating the intracellular signaling pathways associated with modulation of KCC2 trafficking and function. TrkB receptors engage the PLC γ and Shc pathways in adult tissue yielding transcriptional downregulation of KCC2. In contrast, engaging the Shc pathway alone (perhaps early during development) causes upregulation of KCC2 (Rivera et al., 2004). Entry of Ca^{2+} via NMDA receptors causes a decrease in KCC2 activity/expression via dephosphorylation by Ser/Thr phosphatase 1 (PP1) and/or proteolysis by calpain (Lee et al., 2011). In contrast, PKC-mediated phosphorylation promotes KCC2 activity (Bos et al., 2013). KCC2 oligomerization has been suggested to enhance its function (Hartmann and Nothwang, 2014), possibly through tyrosine phosphorylation (Watanabe et al., 2009); however, see Medina et al. (2014). Interactions with other membrane partners (e.g., neto2, kainate receptors; KAR) also appear important to maintain KCC2 oligomerization and function (Ivakine et al., 2013; Mahadevan et al., 2014). Intracellular Zn^{2+} inhibits KCC2 transporter activity (Hershkinkel et al., 2009). The Cl^- -sensitive WNK kinases and their downstream substrate kinases (the SPAK/OSR1 kinases), regulate the inhibitory phosphorylation of the KCCs. Their role is mainly to transduce $[\text{Cl}^-]$, extracellular osmolarity, and cell volume into modulation of volume-activated CCCs (Alessi et al., 2014), but they have been proposed as a target to regulate KCC2 (Kahle et al., 2015).

(D) Summary of intercellular signaling pathways involved in regulation of KCC2. On the left are summarized signaling mechanisms involved in enhancing KCC2 activity, while on the right are those that appear to cause downregulation of KCC2 activity.

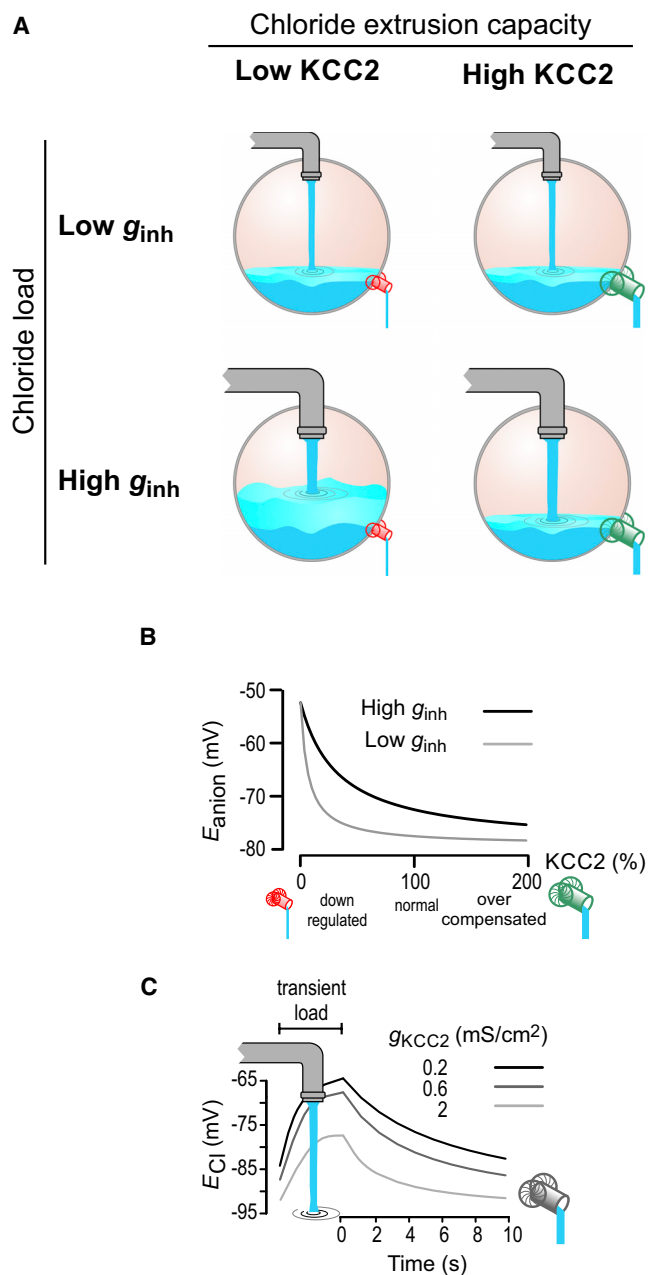


Figure 2. The Dynamics of Cl⁻ Homeostasis

(A) Relationship between Cl⁻ load, KCC2 activity, and [Cl⁻]_i. High [Cl⁻]_i results from a combination of low Cl⁻ extrusion capacity (left) and high Cl⁻ load (bottom). Low Cl⁻ load coupled with low Cl⁻ extrusion capacity (top left) or high Cl⁻ load coupled with high Cl⁻ extrusion capacity (bottom right) will both yield low [Cl⁻]_i.

(B) Consistent with (A), E_{anion} depends on KCC2 levels and Cl⁻ load. Curves plotted here were obtained by simulations in a single compartment conductance-based model that tracked intracellular Cl⁻ according to $d[Cl^-]/dt = (I_{Cl} + I_{KCC2})/(F Vol)$, where F stands the Faraday constant, Vol for the volume of the cell, and I_{KCC2} for the Cl⁻ current through KCC2.

(C) Time course of E_{Cl} recovery after transient Cl⁻ loads also depends on KCC2 level. For details of simulations in (B) and (C), see Doyon et al. (2015).

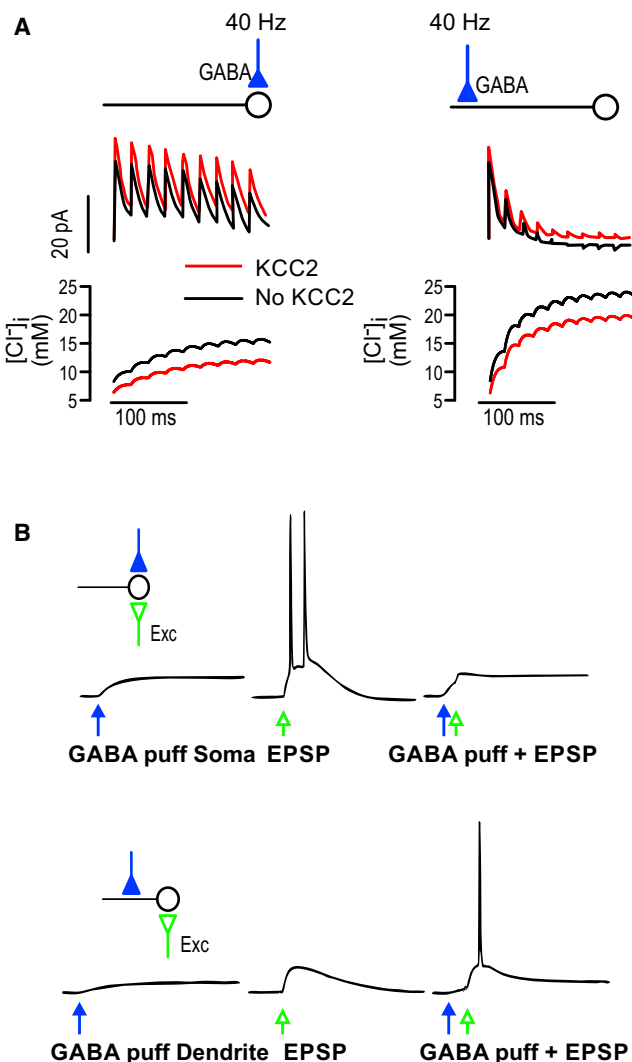


Figure 3. History- and Location-Dependent Failure of Inhibition

(A) Collapse of IPSCs and Cl⁻ accumulation during a 40 Hz barrage of inhibitory input. IPSCs (top) and the associated change in [Cl⁻]_i (middle) for somatic (left) and dendritic (right) input for normal (red) and reduced (black) KCC2 level. Data shown here are from simulations in multicompartment neuron model with electrodiffusion (Doyon et al., 2011).

(B) Impact of intracellular Cl⁻ accumulation on the effects of synaptic inhibition depends on the location of the synaptic input. A slightly depolarizing GABA_A response can be inhibitory if this input is located at the soma, but the same input can be excitatory if dendritically located. This effect boils down to local driving force: when activated GABA_A receptors are in proximity to the excitatory input, local depolarization will enhance the Cl⁻ driving force and thereby increase inhibition, whereas if activated GABA_A receptors are remote from the excitatory input, the Cl⁻ driving force will remain small, and this coupled with bicarbonate efflux will cause net inward current that can contribute to somatic depolarization and excitation. Derived from Gullidge and Stuart (2003) and Jean-Xavier et al. (2007).

disinhibition could be seen as normal (physiological) (e.g., counteracting adaptation in a system where maintaining transmission constant serves a purpose) or detrimental (pathological) (e.g., failure of adaptation in a system where this function serves a computational purpose). Whether activity-dependent disinhibition is beneficial or detrimental ultimately depends on the degree

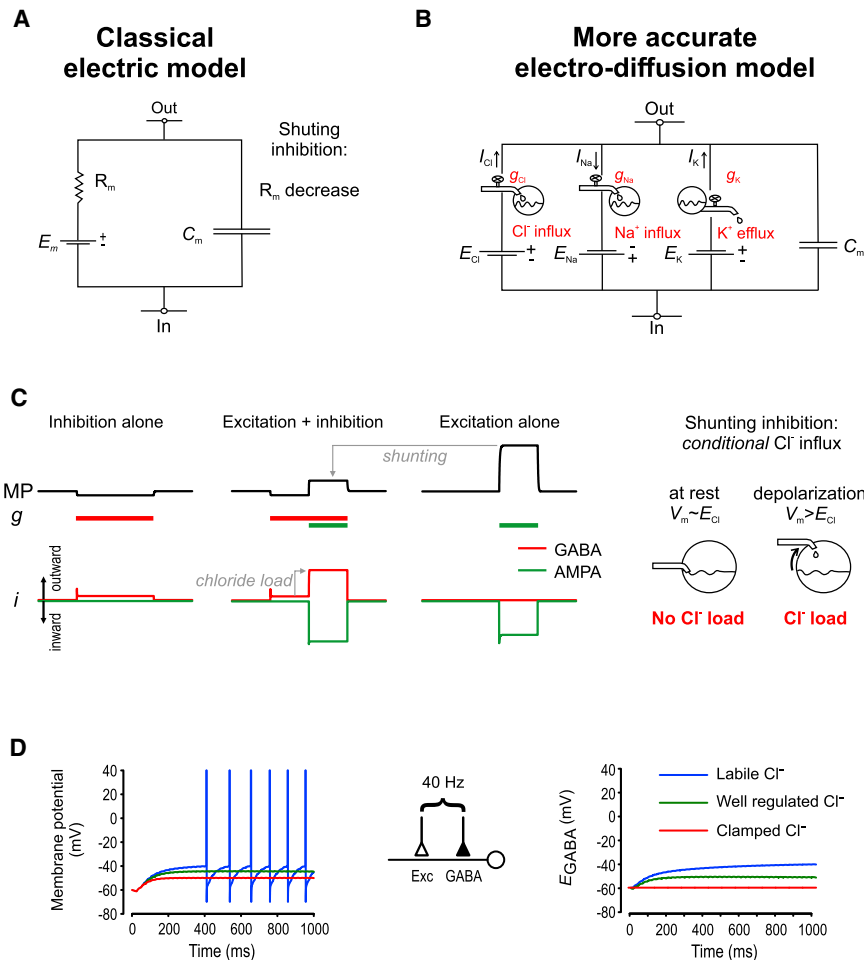


Figure 4. “Shunting” Inhibition Also Imposes a Cl^- Load on Neurons

(A and B) (A) Schematic diagram of the equivalent circuit model often used to describe the cell membrane as an RC circuit. In this simplistic model, all transmembrane conductances are represented as a single resistor associated with a single battery. This depiction is biophysically inaccurate if you consider that different channels are permeable to different ion species and are therefore associated with different batteries (i.e., driving forces). The circuit diagram in (B) more accurately depicts the conductances attributable to different ion species. According to this latter model, shunting inhibition is not due to a nonspecific increase in membrane conductance; instead, it is due to an increase in Cl^- conductance such that outward Cl^- current (i.e., Cl^- influx) can offset the effects of inward cation current.

(C) Simulations in a conductance-based model show that while no net current may be apparent in shunting inhibition mode, significant Cl^- influx (and thus load) occurs when it counteracts an inward (depolarizing) current.

(D) Shunting inhibition can rapidly fail to prevent spiking during sustained dual excitatory and inhibitory input. Data in (D) are from simulations in a multicompartment electrodiffusion model. Under low KCC2 activity (labile Cl^- condition), progressive accumulation of Cl^- occurs despite minimal membrane potential change (“shunting” mode).

atory input originating distal to the inhibitory input and traveling past it toward the soma, will cause a local increase in Cl^- driving force that will, in turn, induce a local hyperpolarizing Cl^- current that shunts the depolarization caused by excitatory synaptic input. Consequently, inhibition of local excitatory input is more resilient

to activity-dependent Cl^- accumulation than is the inhibition of remote excitatory input. Thus, low-frequency inhibitory input distributed across the dendritic tree is more efficient than high-frequency focal inhibitory input; evidence points toward the more efficient arrangement (Doyon et al., 2011; Tamás et al., 1997).

Even “Shunting” Inhibition Can Fail due to Impaired Cl^- Homeostasis

The equivalent circuit model in Figure 4A describes the cell membrane as a resistor and capacitor operating in parallel. According to this classical model, injected current I will charge the capacitor, causing a change in voltage V that follows Ohm's law, $V = IR$, where, in input resistance $R = 1/g$, g is the sum of all transmembrane conductances. The voltage change caused by a depolarizing current can be reduced by introducing a hyperpolarizing current—this is referred to as “hyperpolarizing inhibition.” Alternatively, the voltage change can be reduced by decreasing the input resistance, which is referred to as “shunting inhibition.” Shunting inhibition reduces the input resistance and membrane time constant without causing net current flow, consistent with a simple equivalent circuit model of the membrane (Figure 4A). But Na^+ ions entering through AMPA receptors do not exit through open GABA_A or glycine receptors, contrary to what the term “shunting” might be taken to imply; instead, net current is zero

to which, and extent of time during which, Cl^- extrusion is altered.

Differential Effects on Local versus Remote Excitatory Inputs

Activity-dependent failure of inhibition means that when receiving a train of inhibitory inputs, a dendritic branch will experience hyperpolarization only during the initial phase of the train (Figure 3A, right panels). Hyperpolarization will propagate (notwithstanding attenuation) to the soma, where it can reduce the likelihood of spiking in response to net excitatory input regardless of precisely where (i.e., on which dendrites) the excitatory synapses are located. In contrast, the later phase of the train will be silent (shunting) or even depolarizing, and whereas depolarization can propagate to the soma and cause paradoxical excitation (Gullidge and Stuart, 2003; Jean-Xavier et al., 2007), the so-called “shunting” has only a local effect because there is no voltage differential relative to the soma to encourage current flow (Figure 3B). These effects can also be understood in terms of local driving force: if excitatory synaptic input causes depolarization in proximity to inhibitory synaptic input, the local increase in Cl^- driving force will result in shunting inhibition, but excitatory input that is remote from the inhibitory input will not have the same effect. Therefore, excitatory input near the silent (or even slightly depolarizing) inhibitory input, or excit-

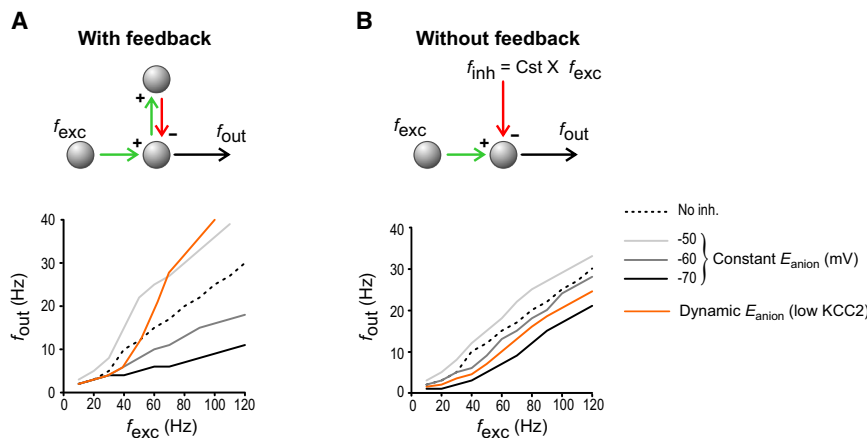


Figure 5. The Impact of Activity-Dependent Disinhibition Varies with Network Topology

Input-output curves for conditions in which inhibition is proportional to excitation (A) or independent of excitation (B). The former connectivity pattern constitutes feedback inhibition. Curves are shown for fixed values of $[Cl^-]_i$, associated with different E_{GABA} and with dynamic $[Cl^-]_i$ associated with low KCC2 activity. Note the compounding effect of disinhibition due to loss of Cl^- extrusion in the case of feedback inhibition, especially when Cl^- dynamics are accounted for. Data are from simulations in a multicompartment electrodiffusion model where f_{exc} is the frequency of excitatory synaptic input and f_{out} is the frequency of spiking in the model neuron (Doyon et al., 2011; Prescott et al., 2006).

because inward current (Na^+ influx) is counterbalanced by outward current (Cl^- influx). What must be appreciated, but is not depicted in the model in Figure 4A, is that different ion channels are permeable to different ion species and are therefore associated with separate batteries (i.e., driving forces), as depicted in Figure 4B. This depiction makes it very clear that shunting occurs when Cl^- influx through GABA_A/glycine channels counterbalances Na^+ influx through AMPA channels (Figure 4C). Even in cases where GABA_A/glycine channels open without initially causing Cl^- flux (e.g., when there is no driving force, i.e., $V = E_{Cl}$), an EPSP will increase the Cl^- driving force, and it is precisely under these conditions that the resulting Cl^- current will “shunt” the EPSP. It logically follows that shunting inhibition involves Cl^- influx and, therefore, imposes a Cl^- load. It also follows that even shunting inhibition relies on the chloride battery, consistent with simulations in Figure 4D showing that shunting inhibition is compromised by depletion of the Cl^- gradient.

Feedback Inhibition Is Most Vulnerable to Activity-Dependent Collapse

As outlined in the Introduction, synaptic inhibition benefits neural information processing by serving many different roles, such as generating oscillations or modulating gain. This multitude of roles is achieved by embedding inhibitory interneurons differently within a neural network. A simple example of this is the case of feedback inhibition in which a neuron forms inhibitory connections with the neuron from which it receives excitatory input (Figure 5A, inset). If Cl^- extrusion is compromised in the excitatory neuron, that neuron will experience less effective inhibition and, consequently, will spike at a higher rate. Due to the network configuration, this will increase the excitatory input onto the inhibitory neuron and, in turn, increase its firing rate. This will increase inhibitory input onto the excitatory neuron, exacerbating Cl^- accumulation. The resulting positive feedback loop can rapidly lead to catastrophic failure of inhibition (Figure 5A) (Doyon et al., 2011). This does not occur when the inhibitory neuron is not embedded within a closed feedback loop (Figure 5B) (Prescott et al., 2006). An important prediction that arises from this is that different inhibitory functions might fail more readily than others, not because certain types of inhibitory interneurons are preferentially compromised, but because the underlying network connectivity causes differentially acceler-

erating Cl^- accumulation in response to input. Specifically, the higher the gain of the negative feedback loop, the greater the risk that mild Cl^- dysregulation could spiral out of control.

The Mismeasure of Cl^- Homeostasis

As already explained, intracellular Cl^- levels depend on the interplay between Cl^- influx through synaptic receptors, efflux through KCC2, and a host of other contributing processes. The resulting relationship between E_{anion} , synaptic input, and KCC2 level is highly nonlinear (Figure 2B). This nonlinear relationship has important implications for how to measure Cl^- regulation. In particular, failing to consider this nonlinearity may cause one to underestimate the true Cl^- dysregulation caused by modest KCC2 reduction and, as a consequence, fail to detect modest reductions in KCC2 and/or falsely exclude such changes as a contributing pathological factor. It is therefore crucial to design future experiments and to reassess past experiments with the following considerations in mind.

Measuring Cl^- Extrusion Capacity under High Cl^- Load Conditions that Exist In Vivo

The strong background synaptic input experienced by neurons in vivo (Destexhe and Paré, 1999; Destexhe et al., 2003) is invariably associated with a strong Cl^- load. If a neuron is tested while experiencing only a weak Cl^- load (i.e., while receiving minimal GABAergic or glycinergic input, such as in a slice preparation), its KCC2 will have excess Cl^- extrusion capacity, which means that changes in E_{anion} only become evident when KCC2 falls well below its normal level (Figure 2A, top). By comparison, smaller reductions in KCC2 level will lead to a change in E_{anion} if the same experiments were carried out under high Cl^- load conditions (Figure 2A, bottom). There are different ways to experimentally impose a large Cl^- load on a neuron. The first is to deliberately dialyze the neuron with pipette solution containing high Cl^- (Figure 6A) (Cordero-Erausquin et al., 2005; DeFazio et al., 2000; Ferrini et al., 2013). In this approach, one can calculate the expected value of E_{anion} based on the assumption that the intracellular Cl^- level equilibrates with the intrapipette Cl^- level; any deviation of the measured E_{anion} value from the expected E_{anion} value reflects how effectively the cell extrudes Cl^- ; the amplitude of the deviation thus represents the Cl^- extrusion capacity. The second method is to subject the cell to a

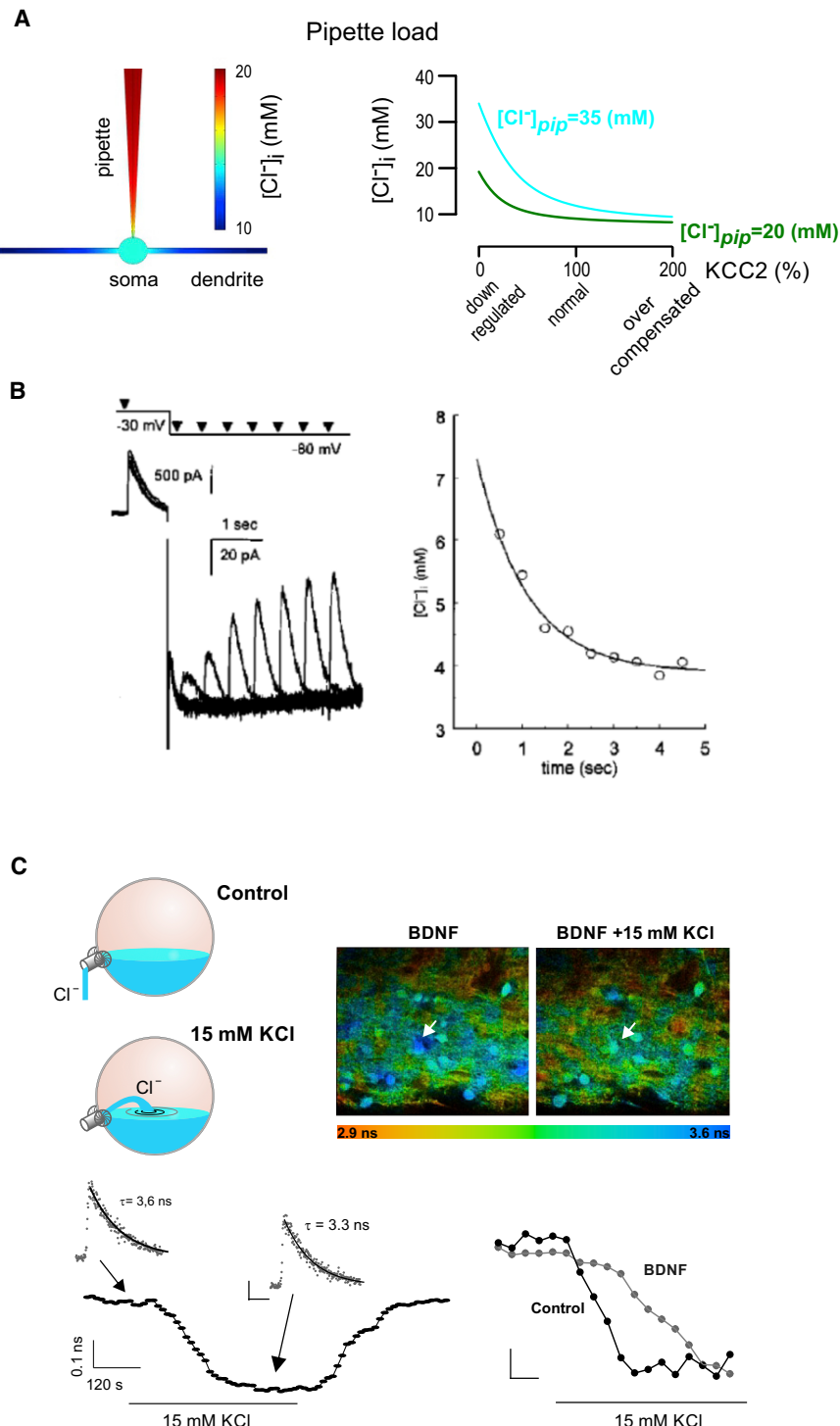


Figure 6. Measuring Changes in Cl^- Homeostasis Must Take Cl^- Dynamics into Account

(A) Imposing a Cl^- load through the pipette in whole-cell patch-clamp recordings yields a much more sensitive method to assess Cl^- extrusion capacity. The value of $[Cl^-]_i$ is inferred from the measured value of E_{anion} and is compared to that expected if $[Cl^-]_i$ equilibrated with the pipette solution ($[Cl^-]_{pip}$) (e.g., Cordero-Erausquin et al., 2005).

(B) Estimating the rate of recovery of $[Cl^-]_i$ from the amplitude of GABA_A synaptic currents elicited at varying intervals after a large conditioning GABA_A current associated with an abrupt jump in membrane potential (from -30 mV to -85 mV) as in Staley and Proctor (1999). The graph on the right illustrates the time course of recovery of $[Cl^-]_i$, inferred from the series of I_{GABA} on the left.

(C) The schematics illustrate how an abrupt change in extracellular $[K^+]$ can be used to trigger a Cl^- transport event. The micrographs show color-coded fluorescence lifetime images of neurons loaded with the Cl^- indicator MQAE in slices. Bottom left: time-lapse recording of Cl^- loading and depletion in the cell bodies of neurons upon switching the extracellular solution to 15 mM KCl and back to control, respectively. Measurements taken every 10 s. Insets: examples of photon distribution histograms fitted to extract lifetimes during the control period (left) and after Cl^- equilibration in 15 mM KCl (right). The slope of the change in fluorescence lifetime reflects the Cl^- transport rate. The time-lapse recording illustrated on the right shows a change in Cl^- transport rate induced by exposing the slice to BDNF. Derived from Ferrini et al. (2013) and Gagnon et al. (2013).

sure Cl^- extrusion capacity is to compute it from the rate at which the I_{GABA} recovers after loading the cell with Cl^- (for example, by triggering a large GABA_A current at depolarized potential and abruptly returning to hyperpolarized potentials). Given that the rate of recovery is related to extrusion capacity, the latter can easily be inferred (Figure 6B) (Staley and Proctor, 1999).

Imaging Transport Rate versus Cl^- Levels

Imaging $[Cl^-]_i$ is gaining popularity as a means to measure Cl^- regulation. However, this approach suffers from the same limitation as electrophysiology in that neglecting Cl^- load conditions can lead to underestimation of modest changes in KCC2 level (see above). But irrespective of $[Cl^-]$, it is possible to directly mea-

barrage of IPSCs (Figure 3A). However, this latter method is confounded by synaptic factors, such as depression, which affect the release of transmitter, although this limitation can be overcome by subtracting Cl^- -independent from Cl^- -dependent attenuation of IPSCs within a barrage of inputs (for examples, see Ferrini et al., 2013; Hewitt et al., 2009). Another way to mea-

sure the rate of Cl^- transport through optical methods by triggering an abrupt change in gradient (by elevating or reducing extracellular $[Cl^-]$ or $[K^+]$ for example (Figure 6C). Notably, it is not possible to do this electrophysiologically because the cotransport process is electroneutral (see “The Ebb and Flow of Chloride”). The availability of ratiometric Cl^- sensors (Arosio

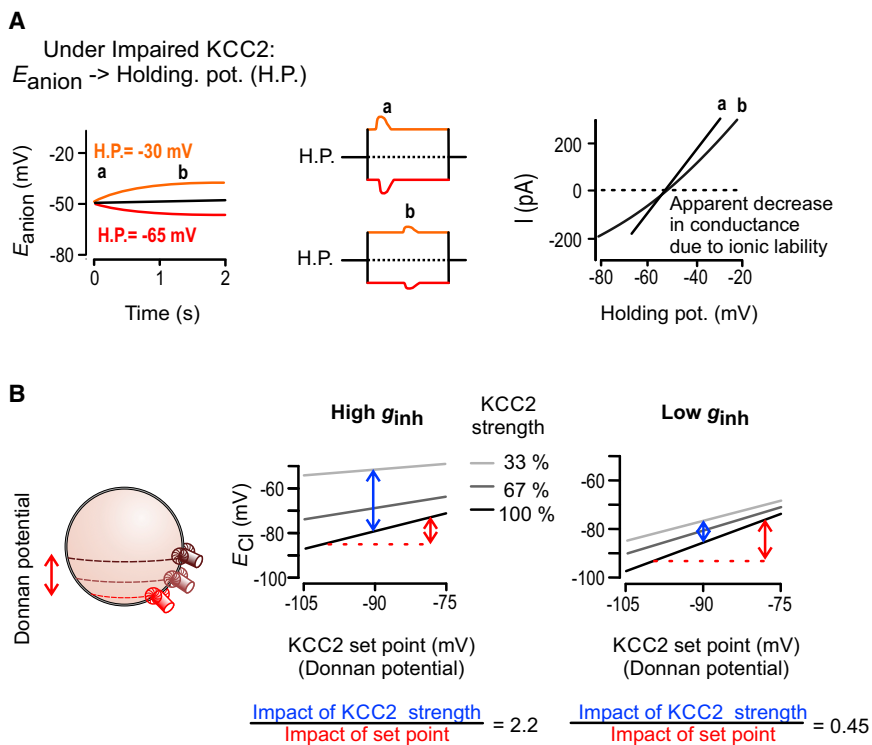


Figure 7. Misunderstanding the Impact of Impaired Cl^- Extrusion

(A) When E_{anion} is measured from the zero point of the I-V plot in a voltage clamp experiment, impaired Cl^- extrusion can give the illusion of a decrease in synaptic conductance as assessed from the slope of the I-V curve. Left: After a step change in holding potential, E_{anion} will change passively due to change in Cl^- driving force that will cause a change in $[\text{Cl}^-]_i$. Middle: the strength of the current response to a stimulation will thus depend on how much Cl^- has accumulated (i.e., when the measurement is taken after the step in holding potential). Right: in (b), the GABA/glycine conductance is underestimated based on the false assumption that Cl^- driving force was unchanged (see Ferrini et al., 2013).

(B) Relative impact of the Donnan effect versus Cl^- extrusion via KCC2 as a function of Cl^- load. The schematic diagram illustrates how the Donnan effect impacts the set point of KCC2 (left). The two graphs illustrate the relative impact of the Donnan effect and KCC2 strength in the case of low g_{inh} (middle) versus high g_{inh} (right), revealing that under low Cl^- load (low g_{inh}), the Donnan effect is the dominant factor determining E_{Cl} , while under heavy Cl^- load (high g_{inh}), KCC2 strength is the main determinant of E_{Cl} . See text for equations used to derive the curves.

et al., 2010; Gagnon et al., 2013; Grimley et al., 2013; Kuner and Augustine, 2000) or fluorescence lifetime approaches (Doyon et al., 2011; Ferrini et al., 2013) is particularly instrumental for these measurements, as they are not confounded by volume changes.

Quantifying Cl^- transport through CCCs remains a major challenge, given that the majority of them are electroneutral, which precludes the direct measurement of ion flux (unlike the case for ion channels and even electrogenic pumps). Moreover, functionally relevant changes in Cl^- concentration are on the order of <20%–50% (in contrast to changes in $[\text{Ca}^{2+}]$ which occur over several orders of magnitudes), making it difficult to find Cl^- -sensitive indicators with the properties needed to precisely measure fluctuations within such a narrow dynamic range (Arosio et al., 2010; Aubé et al., 2014; Coull et al., 2003; Ferrini et al., 2013; Gagnon et al., 2013; Grimley et al., 2013). Techniques that take into account Cl^- dynamics such as Cl^- load protocols and imaging of transport rate provide increased sensitivity. These strategies nevertheless still suffer from the fact that they measure net flux and thus cannot distinguish between changes in activity of the transporters themselves and changes in their expression. Given the emerging key role CCCs play in shaping Cl^- dynamics and the direct consequence of those dynamics for synaptic inhibition, there is a strong impetus to develop new and better approaches to study electroneutral transporters. Perhaps nanoscale or single-molecule imaging approaches will open new perspectives on this front (Chamma et al., 2013).

Illusory Change in Cl^- Conductance

Loss of Cl^- extrusion capacity can also lead to erroneous interpretation of electrophysiological data. For instance, the value of

E_{anion} can be assessed by performing voltage-clamped measurements and observing the transmembrane voltage at which no current is measured (i.e., E_{anion} is the value for which the I-V curve crosses zero). If synaptic conductance is taken to be the slope of this I-V curve, one can observe a decrease in apparent conductance after blocking KCC2 activity (Figure 7A) (Ferrini et al., 2013; Staley et al., 1995; Thompson and Gähwiler, 1989). This decrease in conductance is only apparent because it is based on the assumption that driving force is constant, but that assumption is violated when Cl^- homeostasis is compromised: ion concentration changes (and thus driving force changes) over time as the membrane potential is changed during the I-V protocol (Figure 7A).

The Role of Impermeant Anions on Establishing $[\text{Cl}^-]_i$ Is Diminished in High Cl^- Load Conditions

Glykys et al. (2014) recently argued that the intracellular concentration of impermeant anions ($[\text{A}^-]_i$) is a critical determinant of $[\text{Cl}^-]_i$ via the Donnan effect. The same study also reported that blocking KCC2 had a minimal effect on E_{Cl} , in direct contradiction to a wealth of evidence linking CCCs and Cl^- homeostasis. This has, naturally, stirred debate about how to reconcile the discrepancy (Voipio et al., 2014). We propose a simple explanation based on Cl^- dynamics. As discussed above, $[\text{Cl}^-]_i$ results from the balance of Cl^- influx through GABA_A/glycine channels and its extrusion mainly through KCC2; the value of E_{Cl} is determined by the relative importance of each process. When Cl^- conductance is large, increasing the strength of KCC2 activity will always lead to a sizeable hyperpolarization of E_{Cl} by driving it toward the KCC2 equilibrium point (Figure 7B, left panel). However, in Glykys et al. (2014), measurements were conducted in

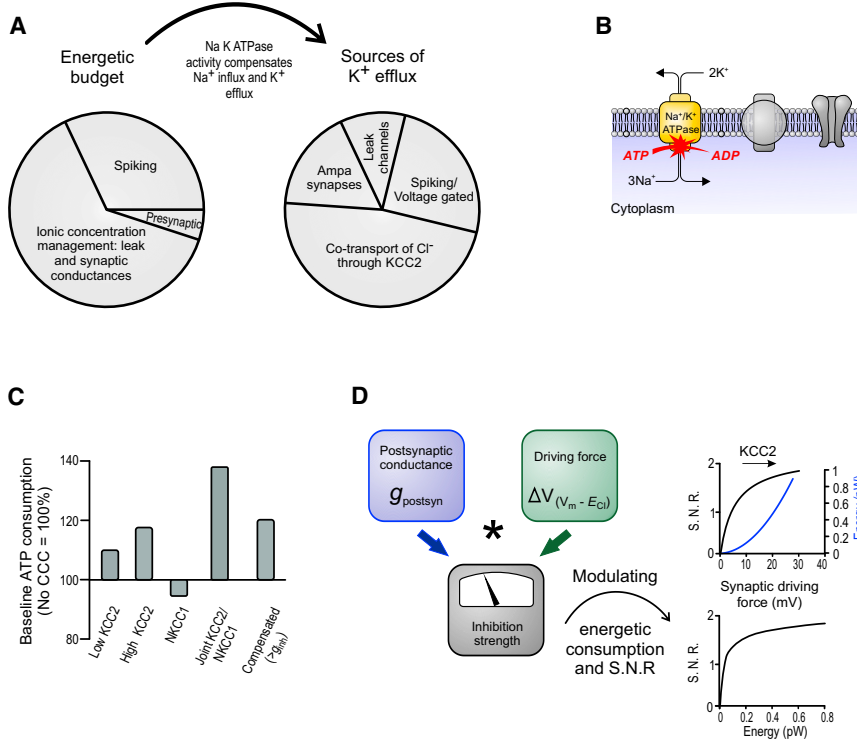


Figure 8. Cl^- Homeostasis, Energy Consumption, and Quality of Synaptic Signaling

(A) Pie chart shows fraction of neuron energy budget of neurons devoted to various neural processes. Maintaining ion concentration is a major expense (left). Relative importance of the different sources of K^+ efflux for a neuron operating in high conductance states and assuming that all synaptic Cl^- influx is balanced by Cl^- extrusion through KCC2 (right). (B) Energy consumption is computed as a function of ATP consumption by the Na^+/K^+ ATPase. (C) Comparison of the energy consumption related to the management of intracellular ion concentrations under various Cl^- regulation scenarios. Calculations assume a low firing rate of 4 Hz, as is typical of most cortical neurons *in vivo*. (D) In contrast to excitatory synapses, Cl^- -regulating mechanisms provide an additional switch to adjust the strength of GABA_A currents. The two switch (conductance and driving force) system (see schematic) allows for differential tuning of the signal to noise ratio (SNR) and energy cost related to a GABA_A synaptic event. Importantly, greater driving force confers a higher SNR (top graph), but this comes with increased energetic costs (bottom graph).

slices with little or no synaptic activity, meaning the Cl^- load was extremely low; as explained above, Cl^- extrusion capacity is best measured under *in vivo*-like Cl^- load conditions. Under artificially low Cl^- load conditions, altering KCC2 activity has little impact on E_{Cl} because of the excess extrusion capacity (Figure 7B, right panel), suggesting instead that determination of E_{Cl} is dominated by the Donnan effect. This can be readily seen from the following:

At equilibrium, $g_{\text{inh}}(V - E_{\text{Cl}}) = g_{\text{KCC2}}(E_{\text{Cl}} - E_{\text{KCC2}})$, and therefore $\partial E_{\text{Cl}} / \partial g_{\text{KCC2}} = g_{\text{inh}}(E_{\text{KCC2}} - V) / (g_{\text{KCC2}} + g_{\text{inh}})^2$. From this we see that E_{Cl} is sensitive to changes in KCC2 activity (g_{KCC2}) only when Cl^- load (g_{inh}) is large. Testing under low Cl^- load conditions will, therefore, lead to gross underestimation of the contribution of KCC2 and overestimation of the contribution of the Donnan effect.

Impact of Cl^- Regulation on Energy Consumption

The idea that evolution leads to constrained optimization is widely accepted, although the exact nature of the optimized quantity or constraints is often not straightforward to identify (Laughlin, 2001; Sarpeshkar, 1998). This starting point has provided useful insights for understanding the neural code, which has been argued to optimize information transfer/storage/processing capacity under conditions in which volume and energy are limited (Laughlin, 2001; Laughlin and Sejnowski, 2003; Varshney et al., 2006). Brain metabolism accounts for 20% of the body's total energy budget (Kety, 1957; Rolfe and Brown, 1997; Sokoloff, 1960), and among the various aspects of neural activity, ion homeostasis is energetically costly (Attwell and Laughlin, 2001) (Figure 8A). This is not surprising when one con-

siders that cortical neurons *in vivo* fire sparsely yet are bombarded by high levels of (balanced) excitatory and inhibitory synaptic input (Destexhe and Paré, 1999; Destexhe et al., 2003; Howarth et al., 2010; Kumar et al., 2008).

Harris et al. (2012) suggested that inhibitory synapses use less energy because the Cl^- reversal is close to the resting membrane potential, but this neglects the fact that Cl^- driving force is increased by excitatory input and that the resulting "shunting" inhibition necessarily involves Cl^- influx (see above and Figure 4); if GABA_A receptor-mediated current must balance AMPA receptor-mediated current, both are energetically costly. Subdividing the energy budget spent on ion homeostasis by comparing the relative contribution of different sources of K^+ efflux (assuming that all Cl^- extrusion occurs through KCC2, that Cl^- conductance via background synaptic input is five times larger than leak conductance measured without background synaptic input, and that the mean firing rate is 4 Hz), reveals that Cl^- regulation via KCC2 is a major source of K^+ efflux (Figure 8A). Since KCC2 is the principal Cl^- extruder, then, under equilibrium conditions, influx of one Cl^- through a GABA_A channel is balanced by efflux of one Cl^- via KCC2, which necessarily involves efflux of one K^+ during the cotransport process. The efflux of that K^+ must be offset by uptake of a K^+ through the Na^+/K^+ ATPase, which carries the energetic cost corresponding to hydrolysis of half an ATP molecule. By comparison, Cl^- loading by NKCC1 has a very different energetic consequence: influx of one Cl^- via NKCC1 is associated with influx of the equivalent of half a sodium ion and half a potassium ion. Given the 3:2 ratio of Na^+ and K^+ transport by the Na^+/K^+ ATPase, the cation cotransport accompanying Cl^- influx via NKCC1 could actually reduce the ATP consumption needed to maintain cation homeostasis (Figure 8B).

But as observed by Attwell and Laughlin (2001), the energetic cost of synaptic inhibition cannot be assessed directly by the number of Na^+ and K^+ shuttled through CCCs. They instead computed the level of Na^+/K^+ ATPase activity needed to maintain equilibrium in terms of membrane potential and (all) ion concentrations, consistent with our argument that Cl^- regulation involves multiple processes that impact other ions. Assuming a high Cl^- load consistent with *in vivo* conditions (Destexhe and Paré, 1999; Destexhe et al., 2003), the type and level of CCC expression are important determinants of energy consumption (Figure 8C). When compared to a scenario with no CCCs, expression of KCC2 increased energy consumption, while the expression of NKCC1 led to modest energy savings by mitigating the K^+ efflux. As expected, coexpression of KCC2 and NKCC1 carries the highest energy costs (Figure 8C) (Staley, 2011).

The argument that the brain has evolved under selective pressure to be energy efficient suggests that the costs of Cl^- extrusion by KCC2 convey benefits for neural coding (see impact of Cl^- extrusion on neural coding in Doyon et al., 2016). Synaptic properties such as the number of postsynaptic channels have been shown to determine the signaling quality of an excitatory synaptic event as well as the energetic cost associated with it (Harris et al., 2012). At GABA_A/glycine synapses, by increasing the driving force, strong KCC2 activity increases the signal-to-noise ratio of synaptic signaling but does so at the expense of using more energy (Figure 8D, where electric work is used as a proxy of energy consumption). In other words, there is a tradeoff between the quality and cost of synaptic inhibition, and although the relationship shown in Figure 8D does not reveal an optimum, this quality/cost relationship likely factors into the bigger picture of how synaptic inhibition balances synaptic excitation to enable efficient neural coding in the context of spiking (Sengupta et al., 2013). Scrimping on Cl^- regulation may be necessary in the face of other competing interests, but how much is too much? There is obviously no simple answer to that question, but one might reasonably speculate that resolving other energetically burdensome problems would allow more energy to be allocated back to Cl^- regulation, thereby restoring the neural processing capabilities.

Pathological Implications and Lessons for Therapeutics

The array of reports associating pathologies with *meta* Cl^- homeostasis is growing at an accelerated pace. These fall into two general categories: (1) evidence of variants of KCC2 transcripts associated with dysfunction of the transporter and (2) evidence of signaling pathways being activated which modulate expression and/or function of CCCs. In the latter case, even if the CCCs are not necessarily the first culprit, the disease may be primarily expressed through impaired Cl^- extrusion, and targeting this defect specifically may be sufficient to restore normal function (see below).

Several neurodevelopmental disorders, such as childhood epilepsy and autism spectrum disorders, appear to involve differential maturation of the NKCC1/KCC2 balance during early development (for reviews, see Ben-Ari et al., 2012; Hadjikhani et al., 2015; Kaila et al., 2014; Lemonnier et al., 2012). Of particular interest is the finding that impaired KCC2 expression or

function is involved in a number of CNS diseases, because this involves an inability to properly regulate and maintain inhibition under the dynamic conditions that characterize neuronal network functioning. Perhaps the most complete set of evidence involving KCC2 dysfunction is in epilepsy and chronic pain.

Depolarizing GABAergic synaptic events underlie interictal-like events in brain slices obtained from patients with temporal lobe epilepsy (Cohen et al., 2002), and downregulation of KCC2 associated with impaired Cl^- extrusion occurs in human temporal lobe epilepsy (Huberfeld et al., 2007) and in neocortical pyramidal neurons of chronically injured epileptogenic neocortex in animal models (Jin et al., 2005). More recently, variants of the KCC2 gene SLC12A5 have been associated with different forms of epilepsy in humans (Kahle et al., 2014b; Puskarjov et al., 2014; Stödberg et al., 2015). Some of the mutations cause a decrease in KCC2 surface expression, a reduction of protein glycosylation, and a partial to complete loss of chloride extrusion (Stödberg et al., 2015).

In neuropathic pain, loss of KCC2 expression/function has been reported in the sensory spinal cord in several animal models (for reviews, see Bonin and De Koninck, 2013; Doyon et al., 2013; Ferrini and De Koninck, 2013; Prescott, 2015). Of particular interest is the finding that BDNF signaling via TrkB receptors appears as the key culprit responsible for the KCC2 downregulation (Figures 1C and 1D) and that blockade of BDNF-TrkB signaling restores normal KCC2 activity (Coull et al., 2005). The latter indicates that KCC2 is maintained at a low level by sustained signaling and that interfering with intracellular regulatory mechanisms (Figure 1C) is a viable approach to reverse the established pathology (Doyon et al., 2013). In injury-associated chronic pain models, BDNF appears to originate from spinal microglia (Figure 1D), while in other syndromes, such as inflammation, BDNF originates from sensory nerves (Figure 1D) (Ferrini and De Koninck, 2013). Even paradoxical hyperalgesia to chronic opiate treatment appears to involve the microglia driven BDNF-TrkB-KCC2 pathway (Ferrini et al., 2013). Yet depending on the model, microglia are not necessarily the only source of BDNF, and KCC2 downregulation may occur independently of BDNF (Lee et al., 2011; Sorge et al., 2015; Zhang and De Koninck, 2008). KCC2 downregulation has been also shown in models of spinal cord injury (Lu et al., 2008) and associated motor spasticity (Boulenguez et al., 2010). Restoring KCC2 activity via modulation of 5HT-2A signaling (Figures 1C and 1D) was shown to attenuate spasticity (Bos et al., 2013), again indicating that restoring Cl^- extrusion can be a viable therapeutic strategy.

Experimental models of drug dependence, where the hedonic response to morphine is blunted after several days of morphine administration, implicate disruption of Cl^- homeostasis in reward pathways (Laviolette and van der Kooy, 2004) and BDNF signaling (Vargas-Perez et al., 2009). Direct involvement of KCC2 downregulation was recently demonstrated in this model and, again, involved microglia-neuron signaling: inhibiting microglial activation restored normal Cl^- transport, dopamine release, and reward response to opiates (Taylor et al., 2016). Of particular interest is the finding that chronic pain recapitulates the disruption of mesolimbic reward circuitry in a fashion similar to that of chronic morphine, again via a neuroimmune-mediated disruption

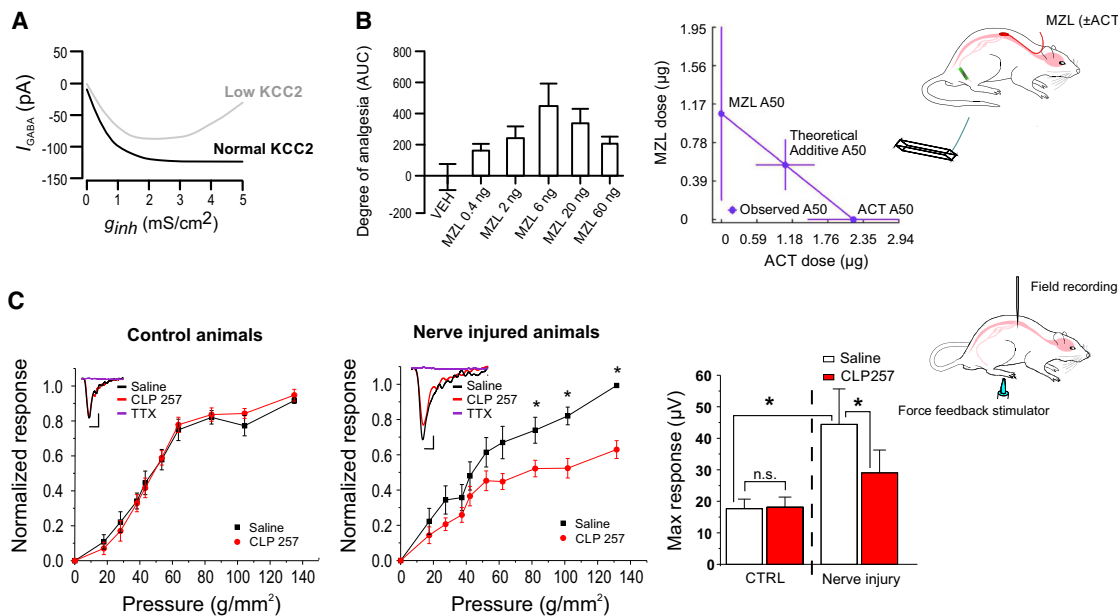


Figure 9. Targeting Cl^- Transport Rather Than Cl^- Conductance for Therapeutics

(A) Theoretical relationships between g_{GABA} and I_{GABA} under normal versus depleted KCC2 activity. Cl^- dynamics cause I_{GABA} to collapse under low-KCC2 conditions, predicting a failure at high conductance levels and limiting the therapeutic window of strategies aimed only at enhancing g_{GABA} . Derived from Doyon et al. (2011).

(B) Left graph: analgesia score as a function of dose of the benzodiazepine midazolam (MZL) administered intrathecally (see diagram in inset) in a model of neuropathic pain (nerve constriction injury illustrated in inset) involving KCC2 hypofunction (AUC, area under the curve). The bell-shaped curve illustrates failure of analgesia at high doses of the GABA_A enhancing drug (MZL). Blocking the carbonic anhydrase with acetazolamide (ACT) to temper the depolarizing HCO_3^- component to GABA_A currents and thus compensate for the collapse in E_{Cl} prevents the failure of analgesia at high doses of MZL (data not shown); consistently, MZL and ACT act synergistically to produce analgesia (right graph). Derived from Asiedu et al. (2010).

(C) Effect of local spinal administration of the KCC2-enhancing drug CLP 257 on amplitude of the field response recorded in superficial spinal dorsal horn in vivo in response to graded mechanical stimulation of the hind foot (see diagram in inset). Enhancing KCC2 had no significant effect on spinal nociceptive input-output function in normal conditions but significantly attenuates enhanced spinal output in experimental model of neuropathic pain. Derived from Gagnon et al. (2013).

of KCC2 activity (Taylor et al., 2015). Impaired Cl^- homeostasis may also play a role in abnormal response to stress. The stress response is mediated by the activity of parvocellular neuroendocrine neurons; GABA_A-mediated inhibition onto these cells is compromised by decreased KCC2 activity in rats submitted to acute restraint stress (Hewitt et al., 2009).

Finally, perturbation of KCC2-mediated Cl^- transport has been suspected to underlie certain psychiatric disorders, such as depression, schizophrenia, and autism spectrum disorders (ASDs). A particular splice variant of KCC2 is increased in dorso-lateral prefrontal cortex tissue of schizophrenia patients but is lower in patients with major depressive disorder (Hyde et al., 2011). Other variants have been reported (Merner et al., 2015; Tao et al., 2012). A decrease in KCC2 in the dorsal lateral pre-frontal cortex was found in subjects with schizophrenia (Sullivan et al., 2015), and a recent study reports association with some splice variants in ASD (Merner et al., 2015).

Given the growing number of diseases in which Cl^- dysregulation is implicated, this pathological mechanism is increasingly recognized as a prime therapeutic target (Ben-Ari et al., 2012; De Koninck, 2007; Gagnon et al., 2013; Kahle et al., 2008, 2014a; Viemari et al., 2011). Numerous pharmacological strategies exist to increase inhibition, but the key is to restore inhibition to normal levels after it has been pathologically diminished. This implies not overcorrecting for the disinhibition and not inadver-

tently enhancing inhibition at synapses where disinhibition has not occurred. An obvious way to increase Cl^- -mediated inhibition is to enhance GABA_A receptor activation through positive allosteric modulators (Knabl et al., 2008), but this approach fails to selectively target disinhibited synapses and invariably increases the Cl^- load, which risks overwhelming diminished Cl^- extrusion capacity if Cl^- dysregulation is the basis for the disinhibition. In this scenario, enhancing GABA_A receptor activation risks precipitating a failure of inhibition or even flipping inhibition into paradoxical excitation as illustrated by computing the value of E_{Cl} as a function of Cl^- load (Figure 9A).

Since the current through GABA_A channels represents the net result of opposing fluxes of Cl^- and HCO_3^- ions, reducing the inward current attributable to HCO_3^- efflux is a reasonable strategy to restore inhibition. One way to attenuate bicarbonate efflux is to block the reaction catalyzed by carbonic anhydrase that replenishes $[\text{HCO}_3^-]$ using acetazolamide (Asiedu et al., 2010; Lee and Prescott, 2015). Not only does this approach prevent GABA from becoming paradoxically excitatory, it also helps curtail the collapse in the Cl^- gradient. This latter effect occurs because bicarbonate efflux depolarizes the membrane potential, which perpetuates the depolarizing shift in E_{anion} and the associated collapse in the Cl^- gradient (Doyon et al., 2011). Consistent with this, acetazolamide was found to help retain the analgesic effects of high doses of the GABA_A-enhancing drug midazolam

(Figure 9B). Yet, despite its usefulness, targeting HCO_3^- homeostasis is likely to have its limitations: while it may prevent the occurrence of depolarizing GABA_A currents, it still does not reverse the impaired Cl⁻ extrusion.

Therapeutic strategies targeting the activity of CCCs themselves are emerging as tools to restore normal ion homeostasis without the unwanted effects associated with an increase in Cl⁻ conductance or inhibitory activity, as described above. The NKCC1 blocker bumetanide is a well-known loop diuretic that has been used in the treatment of heart failure. The impact of this drug in Cl⁻ homeostasis and subsequent excitability in experimental models make it potentially useful to treat some developmental seizure-prone conditions, where it can act synergistically with pro-GABA_A drugs (Dzhala et al., 2005), though experimental studies have also shown limitations of this strategy (Dzhala et al., 2005; Pressler et al., 2015). Bumetanide has also emerged as a potential tool to reduce the severity of autism symptoms (Hadjikhani et al., 2015; Lemonnier et al., 2012). The finding that KCC2 is highly regulated, together with the observation that it can be rescued in pathological conditions, indicates that therapeutic strategies aiming to restore its activity are a viable avenue. Proof of principle that positive modulation of KCC2 function can have therapeutic benefits has recently been provided for analgesia (Gagnon et al., 2013) and treatment of spasticity (Bos et al., 2013) (Figure 9C). A potential concern with this strategy was that increasing KCC2 activity beyond its normal level could lead to excess inhibition. However, in normal conditions, KCC2 already operates near its equilibrium point (Buzsáki et al., 2007) (Figure 2B). Furthermore, the relationship between E_{anion} and KCC2 activity is highly nonlinear such that changes in E_{anion} experience a floor effect, limiting the degree to which inhibition can be enhanced (Doyon et al., 2011, 2013). Consistent with this, enhancing KCC2 was found to have little effect on spinal nociceptive output in normal condition while having a prominent analgesic action in conditions of enhanced excitability associated with spinal downregulation of KCC2 following peripheral nerve injury (Figure 9C) (Gagnon et al., 2013).

Another potential concern of such a strategy is that, because KCC2 extrudes K⁺ together with Cl⁻, it has been proposed that excess KCC2 might lead to overt extracellular K⁺ accumulation, increasing network excitability (Kaila et al., 1997). However, by promoting enhanced inhibition, rescuing KCC2 activity decreases excess firing, which remains the main contributor to extracellular K⁺ accumulation. The net result of increasing KCC2 function thus appears to be a tempering of extracellular K⁺ accumulation (Doyon et al., 2011; Krishnan and Bazhenov, 2011). In summary, targeting electroneutral Cl⁻ transport mechanisms, alone or in conjunction with drugs acting to enhance GABA_A or glycine receptors, is emerging as a therapeutic strategy of choice given the enhanced activity dependence of Cl⁻ accumulation that results from disruption in KCC2 function in a number of CNS pathologies.

Conclusions and Outlook

The inhibition mediated by GABA_A and glycine receptors relies on Cl⁻ moving into the postsynaptic neuron. This is true even in the case of shunting inhibition where the outward current

mediated by Cl⁻ influx offsets (rather than truly shunts) cation-mediated inward current. But whereas inhibition depends directly on Cl⁻ influx, the *continued* efficacy of inhibition depends on Cl⁻ being extruded from the cell so that the electrochemical Cl⁻ gradient does not get depleted. Although other mechanisms contribute, Cl⁻ extrusion occurs primarily via KCC2. Given this reliance on KCC2 and the importance of the dynamic equilibrium of Cl⁻ for synaptic inhibition, it is no wonder that changes in KCC2 are implicated in a number of neurological diseases. But whereas sizeable decreases in KCC2 expression lead to collapse of the Cl⁻ gradient that is obvious from large changes in E_{anion} values, subtler changes in KCC2 expression could go undetected by traditional experimental methods (that most notably neglect Cl⁻ load) yet still have functionally important consequences for synaptic inhibition. For instance, reduced Cl⁻ extrusion capacity increases the likelihood that brief Cl⁻ loads will transiently overwhelm the extrusion mechanisms. This will cause E_{anion} to fluctuate, which will in turn cause the efficacy of synaptic inhibition to fluctuate. The resultant changes in spike rate or timing, or in the frequency of network oscillations, could impact neural coding in important ways especially when inhibitory neurons are imbedded in networks containing inhibitory feedback loops. Subtle changes in KCC2 activity levels might thus underlie clinically important symptoms (Doyon et al., 2016). The take-home message here is that KCC2 levels cannot be thought of as a simple “volume dial” that sets the value of E_{anion} and thereby controls the strength of synaptic inhibition. More sophisticated thinking is required to truly understand what is happening, how to measure it, and how to manipulate it for therapeutic benefit.

ACKNOWLEDGMENTS

The authors acknowledge support from the Canadian Institutes for Health Research (Y.D.K.), the Natural Sciences and Engineering Research Council of Canada (Y.D.K. and S.A.P.), the Fonds de Recherche Québec – Nature et Technologie (N.D.), the French Conseil National de la Recherche Scientifique (L.V.), and Mr. Sylvain Côté for expert assistance with the illustrations. We also thank Frédéric Morneau-Guérin for valuable inputs. S.A.P. is a Canadian Institutes of Health Research New Investigator and Ontario Early Researcher. Y.D.K. holds a Canada Research Chair in Chronic Pain and Related Brain Disorders. This review is dedicated to the memory of Laurent Vinay, who sadly passed away during the revision process of the Review. He was a widely respected scientist, recognized by many for his kindness, humanity, devotion, and scientific insights, together with a remarkable ability to maintain a balanced perspective on controversial issues. His work was also considered transformative, with significant impact on understanding motor development and therapeutics for spasticity after spinal cord injury. Many of the topics and arguments presented in this Review were very dear to him.

REFERENCES

- Alessi, D.R., Zhang, J., Khanna, A., Hochdörfer, T., Shang, Y., and Kahle, K.T. (2014). The WNK-SPAK/OSR1 pathway: master regulator of cation-chloride cotransporters. *Sci. Signal.* 7, re3.
- Arosio, D., Ricci, F., Marchetti, L., Gualdani, R., Albertazzi, L., and Beltram, F. (2010). Simultaneous intracellular chloride and pH measurements using a GFP-based sensor. *Nat. Methods* 7, 516–518.
- Asiedu, M., Ossipov, M.H., Kaila, K., and Price, T.J. (2010). Acetazolamide and midazolam act synergistically to inhibit neuropathic pain. *Pain* 148, 302–308.
- Attwell, D., and Laughlin, S.B. (2001). An energy budget for signaling in the grey matter of the brain. *J. Cereb. Blood Flow Metab.* 21, 1133–1145.

- Aubé, B., Lévesque, S.A., Paré, A., Chamma, É., Kébir, H., Gorina, R., Lécuyer, M.A., Alvarez, J.I., De Koninck, Y., Engelhardt, B., et al. (2014). Neutrophils mediate blood-spinal cord barrier disruption in demyelinating neuroinflammatory diseases. *J. Immunol.* 193, 2438–2454.
- Ben-Ari, Y., Khalilov, I., Kahle, K.T., and Cherubini, E. (2012). The GABA excitatory/inhibitory shift in brain maturation and neurological disorders. *Neuroscientist* 18, 467–486.
- Bonin, R.P., and De Koninck, Y. (2013). Restoring ionotropic inhibition as an analgesic strategy. *Neurosci. Lett.* 557 (Pt A), 43–51.
- Bos, R., Sadlaoud, K., Boulenguez, P., Buttigieg, D., Liabeuf, S., Brocard, C., Haase, G., Bras, H., and Vinay, L. (2013). Activation of 5-HT2A receptors upregulates the function of the neuronal K-Cl cotransporter KCC2. *Proc. Natl. Acad. Sci. USA* 110, 348–353.
- Boulenguez, P., Liabeuf, S., Bos, R., Bras, H., Jean-Xavier, C., Brocard, C., Stil, A., Darbon, P., Cattaert, D., Delpire, E., et al. (2010). Down-regulation of the potassium-chloride cotransporter KCC2 contributes to spasticity after spinal cord injury. *Nat. Med.* 16, 302–307.
- Boulenguez, P., Liabeuf, S., and Vinay, L. (2011). [Reduced neuronal inhibition and spasticity following spinal cord injury]. *Med. Sci. (Paris)* 27, 7–9.
- Brumback, A.C., and Staley, K.J. (2008). Thermodynamic regulation of NKCC1-mediated Cl⁻ cotransport underlies plasticity of GABA(A) signaling in neonatal neurons. *J. Neurosci.* 28, 1301–1312.
- Buzsáki, G., Kaila, K., and Raichle, M. (2007). Inhibition and brain work. *Neuron* 55, 771–783.
- Chamma, I., Heubl, M., Chevy, Q., Renner, M., Moutkine, I., Eugène, E., Poncer, J.C., and Lévi, S. (2013). Activity-dependent regulation of the K/Cl transporter KCC2 membrane diffusion, clustering, and function in hippocampal neurons. *J. Neurosci.* 33, 15488–15503.
- Chance, F.S., Abbott, L.F., and Reyes, A.D. (2002). Gain modulation from background synaptic input. *Neuron* 35, 773–782.
- Cohen, I., Navarro, V., Clemenceau, S., Baulac, M., and Miles, R. (2002). On the origin of interictal activity in human temporal lobe epilepsy *in vitro*. *Science* 298, 1418–1421.
- Cordero-Erausquin, M., Coull, J.A., Boudreau, D., Rolland, M., and De Koninck, Y. (2005). Differential maturation of GABA action and anion reversal potential in spinal lamina I neurons: impact of chloride extrusion capacity. *J. Neurosci.* 25, 9613–9623.
- Coull, J.A., Boudreau, D., Bachand, K., Prescott, S.A., Nault, F., Sík, A., De Koninck, P., and De Koninck, Y. (2003). Trans-synaptic shift in anion gradient in spinal lamina I neurons as a mechanism of neuropathic pain. *Nature* 424, 938–942.
- Coull, J.A., Beggs, S., Boudreau, D., Boivin, D., Tsuda, M., Inoue, K., Gravel, C., Salter, M.W., and De Koninck, Y. (2005). BDNF from microglia causes the shift in neuronal anion gradient underlying neuropathic pain. *Nature* 438, 1017–1021.
- De Koninck, Y. (2007). Altered chloride homeostasis in neurological disorders: a new target. *Curr. Opin. Pharmacol.* 7, 93–99.
- DeFazio, R.A., Keros, S., Quick, M.W., and Hablitz, J.J. (2000). Potassium-coupled chloride cotransport controls intracellular chloride in rat neocortical pyramidal neurons. *J. Neurosci.* 20, 8069–8076.
- Destexhe, A., and Paré, D. (1999). Impact of network activity on the integrative properties of neocortical pyramidal neurons *in vivo*. *J. Neurophysiol.* 81, 1531–1547.
- Destexhe, A., Rudolph, M., and Paré, D. (2003). The high-conductance state of neocortical neurons *in vivo*. *Nat. Rev. Neurosci.* 4, 739–751.
- Doyon, N., Prescott, S.A., Castonguay, A., Godin, A.G., Kröger, H., and De Koninck, Y. (2011). Efficacy of synaptic inhibition depends on multiple, dynamically interacting mechanisms implicated in chloride homeostasis. *PLoS Comput. Biol.* 7, e1002149.
- Doyon, N., Ferrini, F., Gagnon, M., and De Koninck, Y. (2013). Treating pathological pain: is KCC2 the key to the gate? *Expert Rev. Neurother.* 13, 469–471.
- Doyon, N., Prescott, S.A., and De Koninck, Y. (2016). Mild KCC2 hypofunction causes inconspicuous chloride dysregulation that degrades neural coding. *Front. Cell. Neurosci.* 9, 516.
- Dzhala, V.I., Talos, D.M., Sdrulla, D.A., Brumback, A.C., Mathews, G.C., Benke, T.A., Delpire, E., Jensen, F.E., and Staley, K.J. (2005). NKCC1 transporter facilitates seizures in the developing brain. *Nat. Med.* 11, 1205–1213.
- Ferrini, F., and De Koninck, Y. (2013). Microglia control neuronal network excitability via BDNF signalling. *Neural Plast.* 2013, 429815.
- Ferrini, F., Trang, T., Mattioli, T.A., Laffray, S., Del'Guidice, T., Lorenzo, L.E., Castonguay, A., Doyon, N., Zhang, W., Godin, A.G., et al. (2013). Morphine hyperalgesia gated through microglia-mediated disruption of neuronal Cl⁻ homeostasis. *Nat. Neurosci.* 16, 183–192.
- Ford, A., Castonguay, A., Cottet, M., Little, J.W., Chen, Z., Symons-Liguori, A.M., Doyle, T., Egan, T.M., Vanderah, T.W., De Koninck, Y., et al. (2015). Engagement of the GABA to KCC2 signaling pathway contributes to the analgesic effects of A3AR agonists in neuropathic pain. *J. Neurosci.* 35, 6057–6067.
- Gagnon, M., Bergeron, M.J., Lavertu, G., Castonguay, A., Tripathy, S., Bonin, R.P., Perez-Sánchez, J., Boudreau, D., Wang, B., Dumas, L., et al. (2013). Chloride extrusion enhancers as novel therapeutics for neurological diseases. *Nat. Med.* 19, 1524–1528.
- Gilad, D., Shorer, S., Ketzele, M., Friedman, A., Sekler, I., Aizenman, E., and Hershkinkel, M. (2015). Homeostatic regulation of KCC2 activity by the zinc receptor mZnR/GPR39 during seizures. *Neurobiol. Dis.* 81, 4–13.
- Glykys, J., Dzhala, V., Egawa, K., Balena, T., Saponjian, Y., Kuchibhotla, K.V., Bacska, B.J., Kahle, K.T., Zeuthen, T., and Staley, K.J. (2014). Local impermeant anions establish the neuronal chloride concentration. *Science* 343, 670–675.
- Green, D., and Swets, J. (1988). *Signal Detection Theory and Psychophysics* (Los Altos: Peninsul Publishing), pp. 1–505.
- Grimley, J.S., Li, L., Wang, W., Wen, L., Beese, L.S., Hellinga, H.W., and Augustine, G.J. (2013). Visualization of synaptic inhibition with an optogenetic sensor developed by cell-free protein engineering automation. *J. Neurosci.* 33, 16297–16309.
- Gulledge, A.T., and Stuart, G.J. (2003). Excitatory actions of GABA in the cortex. *Neuron* 37, 299–309.
- Hadjikhani, N., Zürcher, N.R., Rogier, O., Ruest, T., Hippolyte, L., Ben-Ari, Y., and Lemonnier, E. (2015). Improving emotional face perception in autism with diuretic bumetanide: a proof-of-concept behavioral and functional brain imaging pilot study. *Autism* 19, 149–157.
- Harris, J.J., Jolivet, R., and Attwell, D. (2012). Synaptic energy use and supply. *Neuron* 75, 762–777.
- Hartmann, A.M., and Nothwang, H.G. (2014). Molecular and evolutionary insights into the structural organization of cation chloride cotransporters. *Front. Cell. Neurosci.* 8, 470.
- Hershkinkel, M., Kandler, K., Knoch, M.E., Dagan-Rabin, M., Aras, M.A., Abramovitch-Dahan, C., Sekler, I., and Aizenman, E. (2009). Intracellular zinc inhibits KCC2 transporter activity. *Nat. Neurosci.* 12, 725–727.
- Hewitt, S.A., Wamsteeker, J.I., Kurz, E.U., and Bains, J.S. (2009). Altered chloride homeostasis removes synaptic inhibitory constraint of the stress axis. *Nat. Neurosci.* 12, 438–443.
- Howarth, C., Peppiatt-Wildman, C.M., and Attwell, D. (2010). The energy use associated with neural computation in the cerebellum. *J. Cereb. Blood Flow Metab.* 30, 403–414.
- Huberfeld, G., Wittner, L., Clemenceau, S., Baulac, M., Kaila, K., Miles, R., and Rivera, C. (2007). Perturbed chloride homeostasis and GABAergic signaling in human temporal lobe epilepsy. *J. Neurosci.* 27, 9866–9873.
- Huguenard, J.R., and Alger, B.E. (1986). Whole-cell voltage-clamp study of the fading of GABA-activated currents in acutely dissociated hippocampal neurons. *J. Neurophysiol.* 56, 1–18.
- Hyde, T.M., Lipska, B.K., Ali, T., Mathew, S.V., Law, A.J., Metitiri, O.E., Straub, R.E., Ye, T., Colantuoni, C., Herman, M.M., et al. (2011). Expression of GABA

- signaling molecules KCC2, NKCC1, and GAD1 in cortical development and schizophrenia. *J. Neurosci.* 31, 11088–11095.
- Isaacson, J.S., and Scanziani, M. (2011). How inhibition shapes cortical activity. *Neuron* 72, 231–243.
- Ivakine, E.A., Acton, B.A., Mahadevan, V., Ormond, J., Tang, M., Pressey, J.C., Huang, M.Y., Ng, D., Delpire, E., Salter, M.W., et al. (2013). Neto2 is a KCC2 interacting protein required for neuronal Cl⁻ regulation in hippocampal neurons. *Proc. Natl. Acad. Sci. USA* 110, 3561–3566.
- Jean-Xavier, C., Mentis, G.Z., O'Donovan, M.J., Cattaert, D., and Vinay, L. (2007). Dual personality of GABA/glycine-mediated depolarizations in immature spinal cord. *Proc. Natl. Acad. Sci. USA* 104, 11477–11482.
- Jin, X., Huguenard, J.R., and Prince, D.A. (2005). Impaired Cl⁻ extrusion in layer V pyramidal neurons of chronically injured epileptogenic neocortex. *J. Neurophysiol.* 93, 2117–2126.
- Kahle, K.T., and Delpire, E. (2015). Kinase-KCC2 coupling: Cl⁻ rheostasis, disease susceptibility, therapeutic target. *J. Neurophysiol.*, in 00865 02015.
- Kahle, K.T., Staley, K.J., Nahed, B.V., Gamba, G., Hebert, S.C., Lifton, R.P., and Mount, D.B. (2008). Roles of the cation-chloride cotransporters in neurological disease. *Nat. Clin. Pract. Neurol.* 4, 490–503.
- Kahle, K.T., Deeb, T.Z., Puskarjov, M., Silayeva, L., Liang, B., Kaila, K., and Moss, S.J. (2013). Modulation of neuronal activity by phosphorylation of the K-Cl cotransporter KCC2. *Trends Neurosci.* 36, 726–737.
- Kahle, K.T., Khanna, A., Clapham, D.E., and Woolf, C.J. (2014a). Therapeutic restoration of spinal inhibition via druggable enhancement of potassium-chloride cotransporter KCC2-mediated chloride extrusion in peripheral neuropathic pain. *JAMA Neurol.* 71, 640–645.
- Kahle, K.T., Merner, N.D., Friedel, P., Silayeva, L., Liang, B., Khanna, A., Shang, Y., Lachance-Touchette, P., Bourassa, C., Levert, A., et al. (2014b). Genetically encoded impairment of neuronal KCC2 cotransporter function in human idiopathic generalized epilepsy. *EMBO Rep.* 15, 766–774.
- Kahle, K.T., Khanna, A.R., Alper, S.L., Adragna, N.C., Lauf, P.K., Sun, D., and Delpire, E. (2015). K-Cl cotransporters, cell volume homeostasis, and neurological disease. *Trends Mol. Med.* 21, 513–523.
- Kaila, K. (1994). Ionic basis of GABA receptor channel function in the nervous system. *Prog. Neurobiol.* 42, 489–537.
- Kaila, K., Lamsa, K., Smirnov, S., Taira, T., and Voipio, J. (1997). Long-lasting GABA-mediated depolarization evoked by high-frequency stimulation in pyramidal neurons of rat hippocampal slice is attributable to a network-driven, bicarbonate-dependent K⁺ transient. *J. Neurosci.* 17, 7662–7672.
- Kaila, K., Price, T.J., Payne, J.A., Puskarjov, M., and Voipio, J. (2014). Cation-chloride cotransporters in neuronal development, plasticity and disease. *Nat. Rev. Neurosci.* 15, 637–654.
- Kety, S.S. (1957). The cerebral circulation in man. *Triangle* 3, 47–52.
- Khubieh, A., Ratté, S., Lankarany, M., and Prescott, S.A. (2015). Regulation of cortical dynamic range by background synaptic noise and feedforward inhibition. *Cereb. Cortex*. Published online July 24, 2015. <http://dx.doi.org/10.1093/cercor/bhv157>.
- Knabl, J., Witschi, R., Hösl, K., Reinold, H., Zeilhofer, U.B., Ahmadi, S., Brockhaus, J., Sergejeva, M., Hess, A., Brune, K., et al. (2008). Reversal of pathological pain through specific spinal GABA receptor subtypes. *Nature* 451, 330–334.
- Krishnan, G.P., and Bazhenov, M. (2011). Ionic dynamics mediate spontaneous termination of seizures and postictal depression state. *J. Neurosci.* 31, 8870–8882.
- Kumar, A., Schrader, S., Aertsen, A., and Rotter, S. (2008). The high-conductance state of cortical networks. *Neural Comput.* 20, 1–43.
- Kuner, T., and Augustine, G.J. (2000). A genetically encoded ratiometric indicator for chloride: capturing chloride transients in cultured hippocampal neurons. *Neuron* 27, 447–459.
- Laughlin, S.B. (2001). Energy as a constraint on the coding and processing of sensory information. *Curr. Opin. Neurobiol.* 11, 475–480.
- Laughlin, S.B., and Sejnowski, T.J. (2003). Communication in neuronal networks. *Science* 301, 1870–1874.
- Lavoie, S.R., and van der Kooy, D. (2004). GABA_A receptors signal bidirectional reward transmission from the ventral tegmental area to the tegmental pedunculopontine nucleus as a function of opiate state. *Eur. J. Neurosci.* 20, 2179–2187.
- Lee, K.Y., and Prescott, S.A. (2015). Chloride dysregulation and inhibitory receptor blockade yield equivalent disinhibition of spinal neurons yet are differentially reversed by carbonic anhydrase blockade. *Pain* 156, 2431–2437.
- Lee, H.H., Deeb, T.Z., Walker, J.A., Davies, P.A., and Moss, S.J. (2011). NMDA receptor activity downregulates KCC2 resulting in depolarizing GABA_A receptor-mediated currents. *Nat. Neurosci.* 14, 736–743.
- Lemonnier, E., Degrez, C., Phelep, M., Tyzio, R., Josse, F., Grandgeorge, M., Hadjikhani, N., and Ben-Ari, Y. (2012). A randomised controlled trial of bumetanide in the treatment of autism in children. *Transl. Psychiatry* 2, e202.
- Lu, Y., Zheng, J., Xiong, L., Zimmermann, M., and Yang, J. (2008). Spinal cord injury-induced attenuation of GABAergic inhibition in spinal dorsal horn circuits is associated with down-regulation of the chloride transporter KCC2 in rat. *J. Physiol.* 586, 5701–5715.
- Mahadevan, V., Pressey, J.C., Acton, B.A., Uvarov, P., Huang, M.Y., Chevrier, J., Puchalski, A., Li, C.M., Ivakine, E.A., Airaksinen, M.S., et al. (2014). Kainate receptors coexist in a functional complex with KCC2 and regulate chloride homeostasis in hippocampal neurons. *Cell Rep.* 7, 1762–1770.
- Marr, D. (1982). Vision: A Computational Investigation into the Human Representation and Processing of Visual Information (Cambridge: MIT Press), pp. 1–369.
- Medina, I., Friedel, P., Rivera, C., Kahle, K.T., Kourdougli, N., Uvarov, P., and Pellegrino, C. (2014). Current view on the functional regulation of the neuronal K(+)-Cl(−) cotransporter KCC2. *Front. Cell. Neurosci.* 8, 27.
- Merner, N.D., Chandler, M.R., Bourassa, C., Liang, B., Khanna, A.R., Dion, P., Rouleau, G.A., and Kahle, K.T. (2015). Regulatory domain or CpG site variation in SLC12A5, encoding the chloride transporter KCC2, in human autism and schizophrenia. *Front. Cell. Neurosci.* 9, 386.
- Payne, J.A., Rivera, C., Voipio, J., and Kaila, K. (2003). Cation-chloride co-transporters in neuronal communication, development and trauma. *Trends Neurosci.* 26, 199–206.
- Prescott, S.A. (2015). Synaptic inhibition and disinhibition in the spinal dorsal horn. *Prog. Mol. Biol. Transl. Sci.* 131, 359–383.
- Prescott, S.A., and De Koninck, Y. (2003). Gain control of firing rate by shunting inhibition: roles of synaptic noise and dendritic saturation. *Proc. Natl. Acad. Sci. USA* 100, 2076–2081.
- Prescott, S.A., Sejnowski, T.J., and De Koninck, Y. (2006). Reduction of anion reversal potential subverts the inhibitory control of firing rate in spinal lamina I neurons: towards a biophysical basis for neuropathic pain. *Mol. Pain* 2, 32.
- Pressler, R.M., Boylan, G.B., Marlow, N., Blennow, M., Chiron, C., Cross, J.H., de Vries, L.S., Hallberg, B., Hellström-Westas, L., Jullien, V., et al.; NEonatal seizure treatment with Medication Off-patent (NEMO) consortium (2015). Bumetanide for the treatment of seizures in newborn babies with hypoxic-ischaemic encephalopathy (NEMO): an open-label, dose finding, and feasibility phase 1/2 trial. *Lancet Neurol.* 14, 469–477.
- Price, T.J., Cervero, F., and de Koninck, Y. (2005). Role of cation-chloride-cotransporters (CCC) in pain and hyperalgesia. *Curr. Top. Med. Chem.* 5, 547–555.
- Puskarjov, M., Seja, P., Heron, S.E., Williams, T.C., Ahmad, F., Iona, X., Oliver, K.L., Grinton, B.E., Vutskits, L., Scheffer, I.E., et al. (2014). A variant of KCC2 from patients with febrile seizures impairs neuronal Cl⁻ extrusion and dendritic spine formation. *EMBO Rep.* 15, 723–729.
- Raimondo, J.V., Markram, H., and Akerman, C.J. (2012). Short-term ionic plasticity at GABAergic synapses. *Front. Synaptic Neurosci.* 4, 5.
- Ratté, S., and Prescott, S.A. (2011). CIC-2 channels regulate neuronal excitability, not intracellular chloride levels. *J. Neurosci.* 31, 15838–15843.

- Rivera, C., Voipio, J., Thomas-Crusells, J., Li, H., Emri, Z., Sipilä, S., Payne, J.A., Minichiello, L., Saarma, M., and Kaila, K. (2004). Mechanism of activity-dependent downregulation of the neuron-specific K-Cl cotransporter KCC2. *J. Neurosci.* 24, 4683–4691.
- Rivera, C., Voipio, J., and Kaila, K. (2005). Two developmental switches in GABAergic signalling: the K+-Cl⁻ cotransporter KCC2 and carbonic anhydrase CAVII. *J. Physiol.* 562, 27–36.
- Rolfe, D.F., and Brown, G.C. (1997). Cellular energy utilization and molecular origin of standard metabolic rate in mammals. *Physiol. Rev.* 77, 731–758.
- Sarpeshkar, R. (1998). Analog versus digital: extrapolating from electronics to neurobiology. *Neural Comput.* 10, 1601–1638.
- Sengupta, B., Laughlin, S.B., and Niven, J.E. (2013). Balanced excitatory and inhibitory synaptic currents promote efficient coding and metabolic efficiency. *PLoS Comput. Biol.* 9, e1003263.
- Seriès, P., Lorenceau, J., and Frégnac, Y. (2003). The “silent” surround of V1 receptive fields: theory and experiments. *J. Physiol. Paris* 97, 453–474.
- Sokoloff, L. (1960). Quantitative measurements of cerebral blood flow in man. *Methods Med. Res.* 8, 253–261.
- Sorge, R.E., Mapplebeck, J.C., Rosen, S., Beggs, S., Taves, S., Alexander, J.K., Martin, L.J., Austin, J.S., Sotocinal, S.G., Chen, D., et al. (2015). Different immune cells mediate mechanical pain hypersensitivity in male and female mice. *Nat. Neurosci.* 18, 1081–1083.
- Soto-Treviño, C., Thoroughman, K.A., Marder, E., and Abbott, L.F. (2001). Activity-dependent modification of inhibitory synapses in models of rhythmic neural networks. *Nat. Neurosci.* 4, 297–303.
- Staley, K.J. (1994). The role of an inwardly rectifying chloride conductance in postsynaptic inhibition. *J. Neurophysiol.* 72, 273–284.
- Staley, K. (2011). Carts, Horses, and Push-Pull Regulation of EGABA in Neonatal Seizures. *Epilepsy Curr.* 11, 205–208.
- Staley, K.J., and Proctor, W.R. (1999). Modulation of mammalian dendritic GABA(A) receptor function by the kinetics of Cl⁻ and HCO3⁻ transport. *J. Physiol.* 519, 693–712.
- Staley, K.J., Soldo, B.L., and Proctor, W.R. (1995). Ionic mechanisms of neuronal excitation by inhibitory GABA_A receptors. *Science* 269, 977–981.
- Stödberg, T., McTague, A., Ruiz, A.J., Hirata, H., Zhen, J., Long, P., Farabella, I., Meyer, E., Kawahara, A., Vassallo, G., et al. (2015). Mutations in SLC12A5 in epilepsy of infancy with migrating focal seizures. *Nat. Commun.* 6, 8038.
- Sullivan, C.R., Funk, A.J., Shan, D., Haroutunian, V., and McCullumsmith, R.E. (2015). Decreased chloride channel expression in the dorsolateral prefrontal cortex in schizophrenia. *PLoS ONE* 10, e0123158.
- Tamás, G., Buhl, E.H., and Somogyi, P. (1997). Fast IPSPs elicited via multiple synaptic release sites by different types of GABAergic neurone in the cat visual cortex. *J. Physiol.* 500, 715–738.
- Tao, R., Li, C., Newburn, E.N., Ye, T., Lipska, B.K., Herman, M.M., Weinberger, D.R., Kleinman, J.E., and Hyde, T.M. (2012). Transcript-specific associations of SLC12A5 (KCC2) in human prefrontal cortex with development, schizophrenia, and affective disorders. *J. Neurosci.* 32, 5216–5222.
- Taylor, A.M., Castonguay, A., Taylor, A.J., Murphy, N.P., Ghogha, A., Cook, C., Xue, L., Olmstead, M.C., De Koninck, Y., Evans, C.J., and Cahill, C.M. (2015). Microglia disrupt mesolimbic reward circuitry in chronic pain. *J. Neurosci.* 35, 8442–8450.
- Taylor, A.M., Castonguay, A., Ghogha, A., Vayssiére, P., Pradhan, A.A., Xue, L., Mehrabani, S., Wu, J., Levitt, P., Olmstead, M.C., et al. (2016). Neuroimmune regulation of GABAergic neurons within the ventral tegmental area during withdrawal from chronic morphine. *Neuropharmacology* 41, 949–959.
- Thompson, S.M., and Gähwiler, B.H. (1989). Activity-dependent disinhibition. I. Repetitive stimulation reduces IPSP driving force and conductance in the hippocampus in vitro. *J. Neurophysiol.* 61, 501–511.
- Vargas-Perez, H., Ting-A Kee, R., Walton, C.H., Hansen, D.M., Razavi, R., Clarke, L., Bufalino, M.R., Allison, D.W., Steffensen, S.C., and van der Kooy, D. (2009). Ventral tegmental area BDNF induces an opiate-dependent-like reward state in naive rats. *Science* 324, 1732–1734.
- Varshney, L.R., Sjöström, P.J., and Chklovskii, D.B. (2006). Optimal information storage in noisy synapses under resource constraints. *Neuron* 52, 409–423.
- Viemari, J.C., Bos, R., Boulenguez, P., Brocard, C., Brocard, F., Bras, H., Coulon, P., Liabeuf, S., Pearlstein, E., Sadlaoud, K., et al. (2011). Chapter 1—importance of chloride homeostasis in the operation of rhythmic motor networks. *Prog. Brain Res.* 188, 3–14.
- Voipio, J., Boron, W.F., Jones, S.W., Hopfer, U., Payne, J.A., and Kaila, K. (2014). Comment on “Local impermeant anions establish the neuronal chloride concentration”. *Science* 345, 1130.
- Watanabe, M., and Fukuda, A. (2015). Development and regulation of chloride homeostasis in the central nervous system. *Front. Cell. Neurosci.* 9, 371.
- Watanabe, M., Wake, H., Moorhouse, A.J., and Nabekura, J. (2009). Clustering of neuronal K+-Cl⁻ cotransporters in lipid rafts by tyrosine phosphorylation. *J. Biol. Chem.* 284, 27980–27988.
- Williams, J.R., and Payne, J.A. (2004). Cation transport by the neuronal K(+)-Cl(−) cotransporter KCC2: thermodynamics and kinetics of alternate transport modes. *Am. J. Physiol. Cell Physiol.* 287, C919–C931.
- Williams, J.R., Sharp, J.W., Kumari, V.G., Wilson, M., and Payne, J.A. (1999). The neuron-specific K-Cl cotransporter, KCC2. Antibody development and initial characterization of the protein. *J. Biol. Chem.* 274, 12656–12664.
- Wu, H., Che, X., Tang, J., Ma, F., Pan, K., Zhao, M., Shao, A., Wu, Q., Zhang, J., and Hong, Y. (2015). The K(+)-Cl(−) cotransporter KCC2 and chloride homeostasis: potential therapeutic target in acute central nervous system injury. *Mol. Neurobiol.* Published online May 5, 2015.
- Zhang, J., and De Koninck, Y. (2008). Central neuroglial interactions in the pathophysiology of neuropathic pain. In *Functional Chronic Pain Syndromes: Presentation and Pathophysiology*, E.A. Mayer and M.C. Bushnell, eds. (Seattle: IASP Press).